ESTABLISHMENT AND UTILITY OF A MULTI-ENVELOPE PSEUDOVIRUS ASSAY TO IDENTIFY LEAD ANTIVIRAL COMPOUNDS.

By

AARON ADOM MANU

(10997378)

SUBMITTED TO

DEPARTMENT OF BIOCHEMISTRY, CELL, AND MOLECULAR BIOLOGY,

COLLEGE OF BASIC AND APPLIED SCIENCES,

SCHOOL OF BIOLOGICAL SCIENCES,

UNIVERSITY OF GHANA, LEGON

IN PARTIAL FULFILMENT FOR THE AWARD

OF

MASTER OF PHILOSOPHY IN BIOCHEMISTRY

SEPTEMBER 2023

DECLARATION

I, Aaron Adom Manu of the Department of Biochemistry, Cell and Molecular Biology, University of Ghana, do hereby declare that, except for the cited references which have been duly acknowledged, this thesis was duly carried out by me, and the results obtained are the true reflection of the work under the supervision of Dr. Peter Kojo Quashie and Dr. Adwoa Padiki Nartey.

Aaron Adom Manu

Signature: ……. Date: 30/03/2025

(Student)

Dr. Peter Kojo Quashie

Signature: ……. Date: 30/03/2025

(Supervisor)

Dr Adwoa Padiki Nartey

Signature: ……. Date: 02/04/2025

DEDICATION

I dedicate this to the All-Powerful God who has been with me over this entire journey. This is also dedicated to my late father, Mr. Isaac Adom Manu, who was a tremendous source of assistance in every aspect.

ACKNOWLEDGEMENT.

I want to thank my superiors sincerely, Dr Quashie and Dr. Nartey for their support and guidance for this project. I would like to acknowledge the West African Centre for Cell Biology of Infectious Pathogens (WACCBIP), and Cambridge Alborada for funding. I also want to thank Quashie Lab members for their assistance with the task. I also value the assistance that Dr. Irene Amoakoh Owusu and Elikem Kisser provided with the project.

I would like to thank my mum, Mrs. Grace Okyem, and my siblings, Ishmael, Isaac, and Maryenda for their prayers and financial support during my studies.

Finally, I would like to acknowledge the entire Department of Biochemistry, Cell, and Molecular Biology staff at the University of Ghana.

Table of Contents

LIST OF FIGURES

LIST OF TABLES

LIST OF ABBREVIATION

ACE2	Angiotensin-converting enzyme 2
HTS	High Throughput-screening
HIV	Human Immunodeficiency Virus
HEK	Human Embryonic Kidney
RLU	Relative Luminescent unit
EBOV	Ebola Virus
COVID-19	Coronavirus disease 2019
HA	Hemagglutinin
DNA	Deoxyribonucleic Acid
S	Spike
NA	Neuraminidase
Gp120	Glycoprotein 120
Ig	Immunoglobulin
IL	Interleukin
Kb	Kilobase
Nsp	Non-structural protein
SARS-COV-2	Severe acute respiratory coronavirus 2
M	Membrane
LB	Luria Broth
N	Nucleocapsid
RNA	Ribonucleic acid
SARS-CoV	Severe acute respiratory coronavirus
MERS-CoV	Middle east respiratory syndrome coronavirus
TMPRSS2	Transmembrane serine protease 2

ABSTRACT

Background: Viral glycoproteins, attach the virus onto host cell surface and this causes the envelope of virus to fuse with the cell membrane of host. This is necessary in the case for most, if not all, of enveloped viruses to enter the host cell. Despite significant breakthroughs in this sector, identifying and developing effective antiviral medications remains challenging. To tackle newly developing and re-emerging viruses, it is essential to develop a reliable and fast assay that can identify broad-spectrum entry inhibitors that can stop viral entry into host cells.

Methods: To determine which transfection method was best to produce the specific pseudovirus; Lipofectamine, polyethyleneimine (PEI), and Calcium phosphate transfection were employed in producing Marburg, Ebola, and SARS-CoV-2 pseudoviruses. Cytotoxicity assay of the compounds obtained from *Bacillus* and *Streptomyces spp*. was performed on the permissive cell lines (293T and ACE-293 cells) using resazurin (Alamar blue) assay. An inhibition assay was done by using one-tenth of the cytotoxic concentration (CC 50) of the compounds against the various pseudoviruses.

Results: ACE2 HEK293 cell line was produced for SARS-CoV-2 pseudovirus infection. Polyethyleneimine (PEI) was effective in producing Marburg pseudovirus. However, the lipofectamine method was the most effective in producing high pseudovirus titers for SARS-CoV-2 and EBOV-Makona. Resazurin was used in determining the cell toxicity of all 32 compounds against Human Embryonic Kidney (HEK293T) and ACE2 HEK293 cells. The CC 50 of the 32 compounds was determined using a dose-response curve. For the inhibition out of the 32 compounds screened on the 3 different pseudoviruses: 2 compounds inhibited MARV, 5 inhibited EBOV and 5 inhibited SARS-CoV-2 pseudoviral entry.

Conclusion: The plasmids used to produce the pseudoviruses are reliable for pseudovirus production and can be used for viral infectivity and inhibition assays. PEI is effective in producing MARV pseudovirus and lipofectamine is also effective for producing SARS-CoV-

2 and EBOV pseudoviruses. Five compounds showed inhibition against SARS-CoV-2. Compound (30) showed active pan-inhibitory effect against Marburg and Ebola pseudoviruses. The assay was reliable in showing compounds that had some inhibitory activity against all the three pseudoviruses.

Significance: This assay is good for finding formal hit compounds against viral entry of the three viruses used and can also be optimized for other enveloped viruses of concern to screen for entry inhibitors.

CHAPTER ONE

1.0 Introduction

Viruses are ubiquitous microorganisms responsible for a wide range of infections, contributing to significant mortality and economic burden worldwide. They are broadly grouped into enveloped and non-enveloped viruses. Enveloped viruses are distinguished by a lipid bilayer that surrounds the viral capsid, which is derived in part from the host cell membrane and decorated with virus-specific glycoproteins (Navaratnarajah, Warrier, & Kuhn, 2008). These glycoproteins play critical roles during infection by recognizing and attaching to host cell receptors, thereby mediating viral entry (Cosset & Lavillette, 2011). Enveloped viruses include some of the most high-risk pathogens of global concern. Clinically important enveloped viruses include SARS-CoV-2, influenza virus, Marburg virus, Ebola virus, and HIV, all of which are associated with severe diseases that are challenging to treat or manage. Their dependence on surface glycoproteins embedded in their lipid envelopes to mediate receptor recognition, membrane fusion, and host cell entry, provide effective targets for entry inhibitors (Harrison, 2015; Walls et al., 2020). In contrast, non-enveloped viruses utilize capsid proteins to penetrate host cells through mechanisms such as pore formation or endosomal escape, which present fewer accessible molecular targets for natural metabolite-derived inhibitors (Ryu, Kim, & Lee, 2021).

Therapeutic targeting of viral proteins such as polymerases, proteases, and entry-associated glycoproteins has been central to antiviral development. The viral life cycle provides multiple potential points of intervention. For example, SARS-CoV-2 uses its spike protein to bind angiotensin-converting enzyme 2 (ACE2) as its primary receptor, with co-receptors such as TMPRSS2 and cathepsins B and L facilitating entry (Hoffmann et al., 2020; Shang et al., 2020). Influenza viruses rely on hemagglutinin (HA) to attach to host receptors and neuraminidase

(NA) to cleave sialic acid residues, both of which are crucial to infection (Skehel & Wiley, 2000). Similarly, Ebola and Marburg viruses' express glycoproteins that bind multiple receptors including C-type lectins (DC-SIGN, L-SIGN), Tyro3/Axl/Mer (TAM) receptors, and Niemann-Pick C1 protein (Kajihara & Takada, 2015; Ning et al., 2017). HIV employs gp160, which is cleaved into gp120 and gp41, to mediate sequential binding to CD4 and CCR5, followed by fusion and entry into host CD4+ lymphocytes.

Human Immunodeficiency Virus (HIV) also invades and uses the surface glycoprotein gp160, which is made up of gp120 and gp41, as its "key" to enter CD4 lymphocytes. The virus initiates entry by binding its gp120 envelope protein to CD4 receptors on the host cell surface, followed by interaction with the CCR5 co-receptor.

These examples illustrate that viral entry pathways represent an attractive first line of intervention for antivirals. Entry inhibitors block infection at its earliest stage, preventing viral replication, limiting spread, and potentially reducing cytotoxicity. Drugs targeting entry steps, such as attachment, co-receptor binding, and membrane fusion, are already under development (Singh & Chauthe, 2011), with some investigated as microbicides to prevent sexual transmission (Farr et al., 2013).

Natural microbial metabolites are increasingly being investigated for their antiviral potential. Secondary metabolites from bacteria and fungi have shown inhibitory activities against viral infections, underscoring the need for systematic evaluation of these compounds. Additionally, many microbial secondary metabolites, including lipopeptides and flavonoids, exert their antiviral activity by disrupting lipid membranes or blocking glycoprotein–receptor interactions, making them particularly relevant for enveloped virus inhibition (Lin et al., 2021; Yu et al., 2023). Focusing on enveloped viruses therefore provides a rational link between the

structural vulnerabilities of these pathogens and the bioactive potential of natural products, while also directly addressing urgent global health threats posed by emerging and re-emerging enveloped viruses. A key step in such research is the use of pseudovirus assays, which mimic viral entry without requiring high-level biosafety facilities. Pseudotyping allows the expression of viral glycoproteins on the surface of non-replicating reporter viruses, enabling safe, high-throughput drug screening (Simmons et al., 2004; Wool-Lewis & Bates, 1998).

Originally developed for HIV research, pseudovirus systems have since been adapted to multiple viruses including SARS-CoV-2, Ebola virus, and Marburg virus. This provides a versatile and safer approach to studying viral entry and screening candidate inhibitors at biosafety level 2. In this study, pseudovirus systems for SARS-CoV-2, Ebola virus, and Marburg virus were established and used to evaluate natural compounds derived from Bacillus and Streptomyces species. The ultimate goal was to identify molecules with selective inhibitory activity against viral entry, contributing to potential prophylactic and therapeutic strategies for emerging and re-emerging enveloped viruses.

1.1 Problem Statement

Viral emergence and re-emergence, like the current COVID-19 pandemic, is a major threat to public health worldwide. The discovery and creation of efficient antiviral therapy continue to remain difficult despite major advancements in this field. Also, the diversity of viruses, including their various envelope proteins, receptors, and entry methods, makes the identification and development of entry inhibitors difficult. A safe and sensitive assay that can allow for rapid screening of broad-spectrum entry inhibitors of viruses is crucial in the fight against newly emerging and reemerging viruses.

1.2 Rationale

Enveloped viruses pose significant threats to public health. The emergence and re-emergence of these viruses including SARS-Cov2, Ebola, Marburg are of great public health concern. The development of broad-spectrum entry inhibitors offers a promising strategy to mitigate their spread (Geraghty, Aliota, & Bonnac, 2021). Since viral entry constitutes an early and crucial phase of infection, its inhibition can prevent replication before resistance emerges, thereby reducing both the severity of the disease and its transmission (Pattnaik & Chakraborty, 2020). Nevertheless, the identification of such inhibitors relies on dependable assays capable of rapidly and safely evaluating candidate compounds. A pseudoviral panel assay facilitates this process, enabling scalable and efficient screening of microbial metabolites with potential antiviral properties.

1.3 Aim

The aim of this study was to establish a suitable assay for screening entry inhibitors of SARS-CoV-2, Ebola virus, and Marburg virus.

1.4 Objectives

The specific objectives of this study were to;

1. Establish pseudoviruses using lentiviral backbones for SARS-CoV-2, Ebola virus, and Marburg virus.
2. Apply the pseudovirus assay in screening microbial metabolites derived from Bacillus and Streptomyces species for their ability to inhibit viral entry.

CHAPTER TWO

2.0 Literature review

2.1 Antivirals and need for screening assays.

The development of antiviral drugs has long been challenged by viral resistance (De Clercq, 2006). Effective drug discovery relies on assays capable of identifying compounds with antiviral activity and elucidating their mechanisms of action (Shyr et al., 2021). Screening assays thus play a central role in identifying lead compounds for optimization and further development. Among the most promising approaches for studying viral entry and evaluating inhibitors are pseudovirus-based systems, which allow high-throughput and biosafe screening (Xiang et al., 2022).

Microorganisms such as bacteria and fungi are well-known producers of bioactive metabolites. These natural products have historically yielded antibiotics (e.g., penicillin) and antifungal agents (e.g., amphotericin B, fluconazole), and they continue to serve as a rich source of novel drug candidates (Ghannoum & Rice, 1999; Frediansyah et al., 2022).

2.2 Tools for Antiviral Screening

Antiviral screening is the process of testing potential compounds for their ability to inhibit viral replication or infectivity. There are several methods used in antiviral screening, including: High-throughput screening (HTS) approach which involves testing large libraries of compounds against viruses in vitro (outside of a living organism) using automated systems (Ayon, 2023). HTS allows for the testing of an array of compounds in a moderately short amount of time. This approach is widely used by pharmaceutical companies to identify potential antiviral compounds. The use of *in silico* screening approach by computer algorithms to simulate the interaction between potential compounds and viral targets (Oliveira, Silva, Maia, Silva, & Taranto, 2023). To minimize *in vitro testing*, *in silico* screening scientists can

be used to filter candidate compounds**.** There are also, phenotypic screening approach involves testing compounds against viruses in a living organism or cell culture system (Etzion & Muslin, 2009; Rietdijk et al., 2021). The goal is to identify compounds that have antiviral activity in a more realistic setting. The use of repurposing approach involves testing existing drugs or compounds that have been approved for other uses against viral infections (Martinez, 2022; Trivedi, Mohan, & Byrareddy, 2020). This approach can be faster and more cost-effective than developing new compounds from scratch (Krishnamurthy, Grimshaw, Axson, Choe, & Miller, 2022). Antiviral screening typically involves several stages of testing, including initial screening, hit validation, lead optimization, and preclinical testing. This process can take several years and requires a considerable number of resources and expertise. However, successful antiviral screening can lead to the development of new drugs that can help prevent or treat viral infections.

2.3 The use of phenotypic screening model; Pseudoviruses.

The development of pseudovirus systems has provided a versatile and safer alternative to working with highly pathogenic viruses that require biosafety level-3 or level-4 facilities. Several pseudovirus designs have been established depending on the viral family of interest, with the most widely used backbones derived from lentiviruses (such as HIV-1), vesicular stomatitis virus (VSV), and murine leukemia virus (MLV). These backbones can be engineered to express the envelope glycoproteins of target viruses such as SARS-CoV-2, Ebola virus, or Marburg virus, thereby faithfully mimicking the viral entry process while lacking the capacity for replication (Hu et al., 2020; Chen et al., 2017). The choice of pseudovirus backbone influences assay performance: HIV- and MLV-based pseudoviruses are widely used for luciferase or GFP reporter assays because of their sensitivity and adaptability, whereas VSV-

based systems often generate higher titres but are less flexible for high-throughput screening (Yang et al., 2021).

Early applications in filovirus research successfully generated HIV-based Ebola and Marburg pseudoviruses to establish neutralization assays under BSL-2 conditions, which became essential for the preclinical evaluation of antivirals and vaccines (Chen & Guo, 2015). More recently, optimized SARS-CoV-2 pseudovirus systems using codon-optimized spike constructs and dual-reporter vectors have further improved reproducibility and throughput in antiviral testing (Rudometova et al., 2022; Hu et al., 2020). The utility of pseudoviruses extends beyond coronaviruses and filoviruses; they have also been used to model the entry process of influenza, HIV, and henipaviruses, enabling the discovery of inhibitors targeting viral envelope proteins such as SARS-CoV-2 spike, influenza hemagglutinin and neuraminidase, and HIV Env (Haim et al., 2009; Nie et al., 2020). One notable example is the use of VSV pseudotypes to study Ebola virus entry, which contributed to the identification of promising inhibitors, including the small molecule TAK-779 and the monoclonal antibody KZ52 (Côté et al., 2011).

Despite their advantages, pseudovirus-based assays are not without limitations. Because pseudoviruses are restricted to mimicking the entry stage, they cannot recapitulate the complete viral life cycle, including replication and spread, and therefore may miss inhibitors acting at later stages of infection (Hu et al., 2020). Furthermore, there is the potential for false positives, as the simplified system does not fully portray the complexity of virus–host interfaces that occur during a natural infection. Nevertheless, pseudoviruses remain a powerful tool for antiviral screening, particularly at the early stages of drug discovery when rapid, safe, and scalable assays are required. The development of pseudoviral panels, such as the one employed

in this study, holds promise for identifying broad-spectrum antiviral candidates while mitigating biosafety challenges associated with authentic viruses.

2.4 Severe Acute Respiratory Syndrome Virus-2 (SARS-CoV-2)

SARS-CoV-2, initially recognized in Wuhan, China, in December 2019, is a member of the Coronaviridae family of enveloped positive-sense RNA viruses. (Zhu et al., 2020; WHO, 2020). It is classified within the betacoronavirus genus, sharing 79% genomic similarity with SARS-CoV and approximately 50% with MERS-CoV (Lu et al., 2020). The virus encodes structural proteins (spike, envelope, membrane, nucleocapsid) and several accessory proteins that contribute to pathogenicity (Chan et al., 2020).

The spike glycoprotein, a trimeric transmembrane protein, mediates viral attachment to ACE2 and subsequent membrane fusion, assisted by proteases such as TMPRSS2. It consists of two subunits: S1, which contains the receptor-binding domain (RBD), and S2, which contains the fusion machinery (Naqvi et al., 2020). Structural rearrangements following receptor binding trigger fusion of viral and host membranes (Figure 2.1). The close similarity between SARS-CoV and SARS-CoV-2 spike proteins underscores the importance of targeting spike in antiviral development.

The replication cycle begins with ACE2-mediated binding, followed by entry via endocytosis or direct membrane fusion (Xia et al., 2020). Viral RNA acts as a template for translation of polyproteins, which are processed into nonstructural proteins including the RNA-dependent RNA polymerase (Gordon et al., 2020). Newly formed virions are assembled in the ER–Golgi intermediate compartment and released by exocytosis (Stertz et al., 2007) (figure 2.2).

Pathogenesis involves infection of respiratory epithelial cells and broad organ involvement, reflecting ACE2 distribution across multiple tissues. Severe disease often results from hyperinflammatory responses and cytokine storm, leading to tissue injury, multi-organ dysfunction, and coagulopathy (Blanco-Melo et al., 2020; Mangalmurti & Hunter, 2020).

Management strategies include antiviral drugs such as remdesivir, nirmatrelvir–ritonavir, and molnupiravir, alongside supportive care and vaccination (Liu et al., 2020). Non-pharmaceutical interventions such as masking and hygiene remain important in preventing spread.

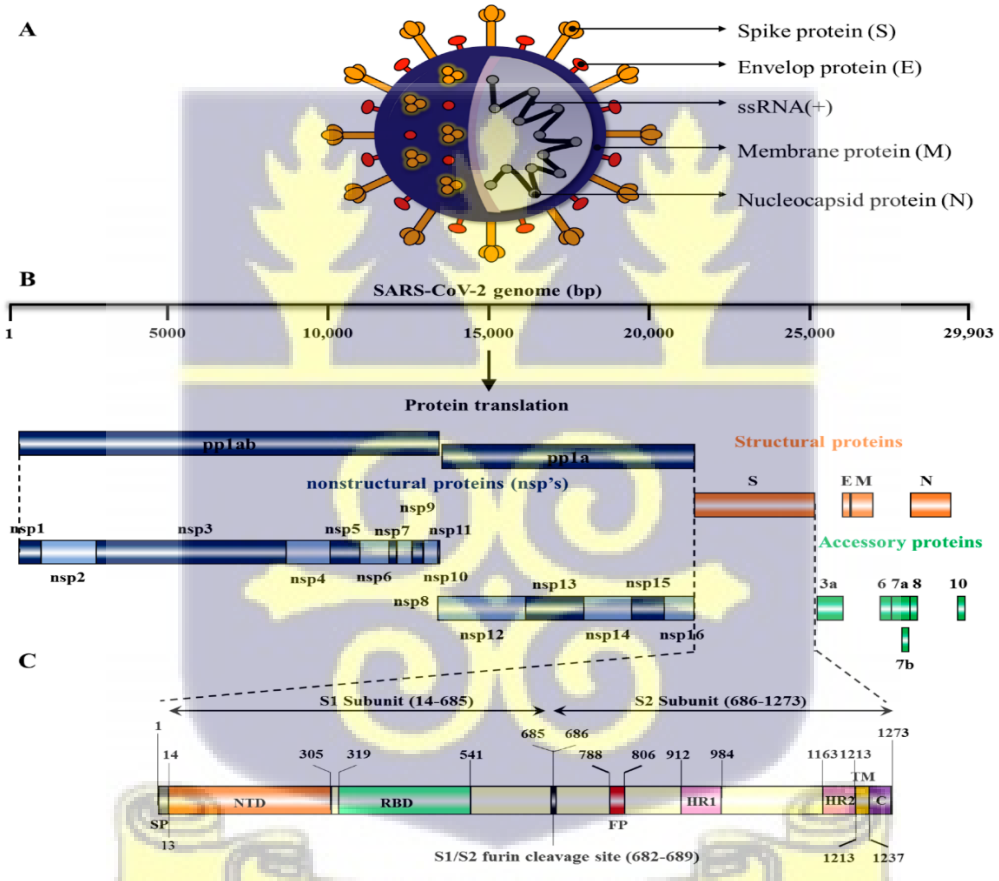

Figure 2. 1: SARS-CoV-2 particle structure and genome organization (Tulimilli et al., 2022).

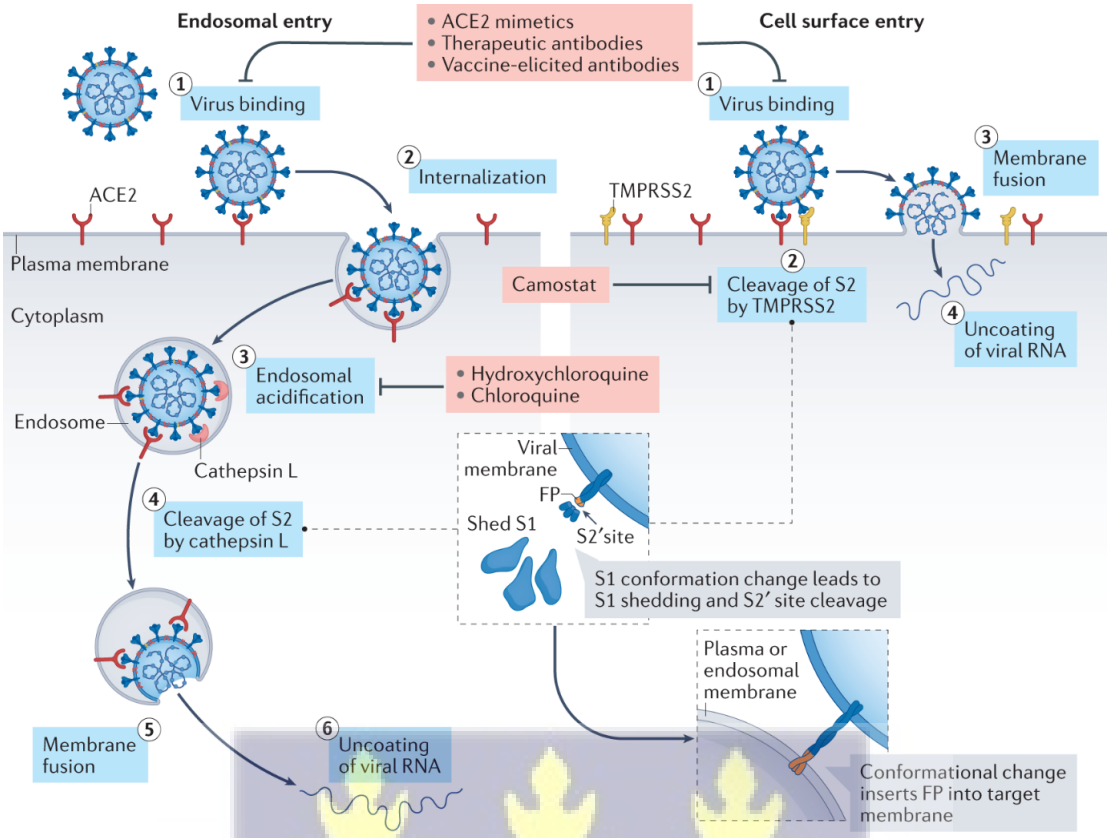

Figure 2. 2: Life cycle of SARS-CoV-2 in host cell (Jackson, Farzan, Chen, & Choe, 2022).

2.5 Ebola virus

Ebola virus, a member of the Filoviridae family, is a filamentous negative-sense RNA virus responsible for Ebola virus disease (EVD), characterized by hemorrhagic fever and high mortality (Feldmann & Geisbert, 2011; Baize et al., 2014). Five species have been identified, with Zaire, Sudan, and Bundibugyo ebolaviruses responsible for most outbreaks (Malvy et al., 2019).

The genome encodes structural proteins including glycoproteins (GP, sGP, ssGP), nucleoprotein, VP24, VP30, VP35, VP40, and polymerase L (figure 2.3a). GP mediates host receptor interaction and macropinocytosis-mediated entry, with Niemann-Pick C1 protein acting as a critical intracellular receptor (Wool-Lewis & Bates, 1998). VP24 and VP35 interfere with interferon signaling, facilitating immune evasion (figuren2.3b).

EBOV pathogenesis involves infection of dendritic cells, macrophages, and monocytes, triggering massive cytokine release and immune dysregulation. Histopathological features include hepatocellular necrosis, lymphoid depletion, and disseminated intravascular coagulation (Geisbert et al., 2000; Zaki & Goldsmith, 1999).

Management remains largely supportive, but advances in monoclonal antibodies (e.g., Inmazeb, Ebanga) and antivirals such as favipiravir show promise (Furuta et al., 2013; Winkler & Koepsell, 2015).

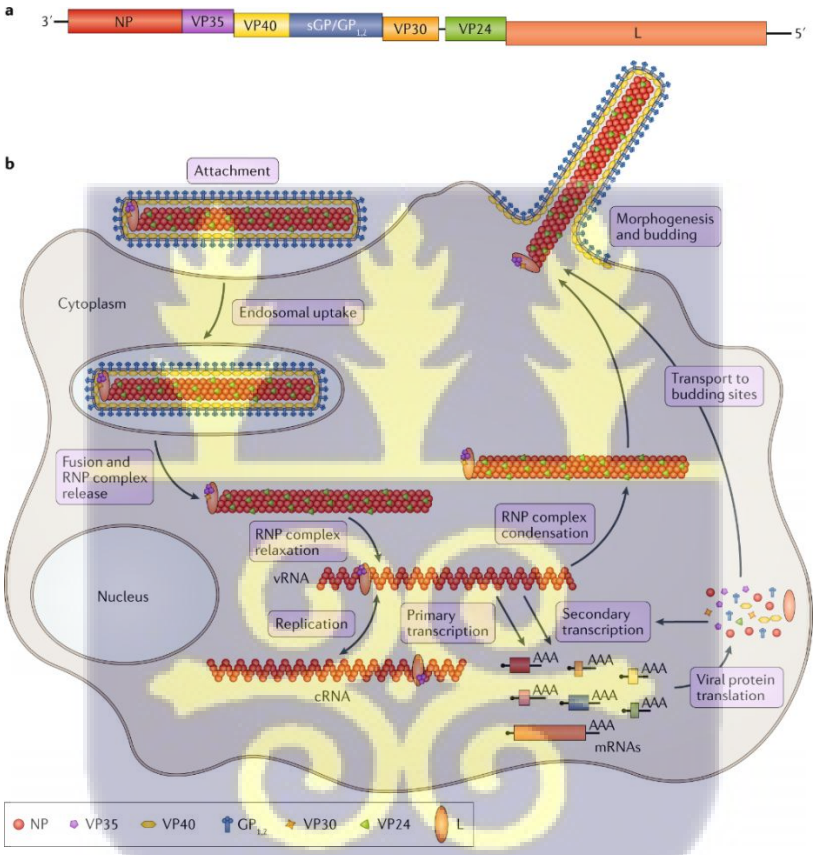

Figure 2. 3: Genome structure and life cycle of EBOV (Hoenen, Groseth, & Feldmann, 2019)

2.6 Marburg virus

Marburg virus, another Filoviridae member, causes Marburg virus disease (MVD), a severe haemorrhagic fever. It is transmitted from fruit bats (Rousettus aegyptiacus) to humans, with secondary transmission via contact with infected body fluids (Kortepeter et al., 2020).

The genome encodes seven proteins, including GP, VP24, VP35, VP40, nucleoprotein, and polymerase L (figure 2.4b). GP mediates host attachment and entry, similar to EBOV. The disease progresses through early febrile, organ dysfunction, and late hemorrhagic phases (Martini, 1971). Mortality rates remain high, with multiorgan failure being the major cause of death (Borchert et al., 2007).

Management relies on supportive care, as no approved antivirals exist. Preventive strategies include avoiding exposure to bats and strict infection control during outbreaks (Islam et al., 2023).

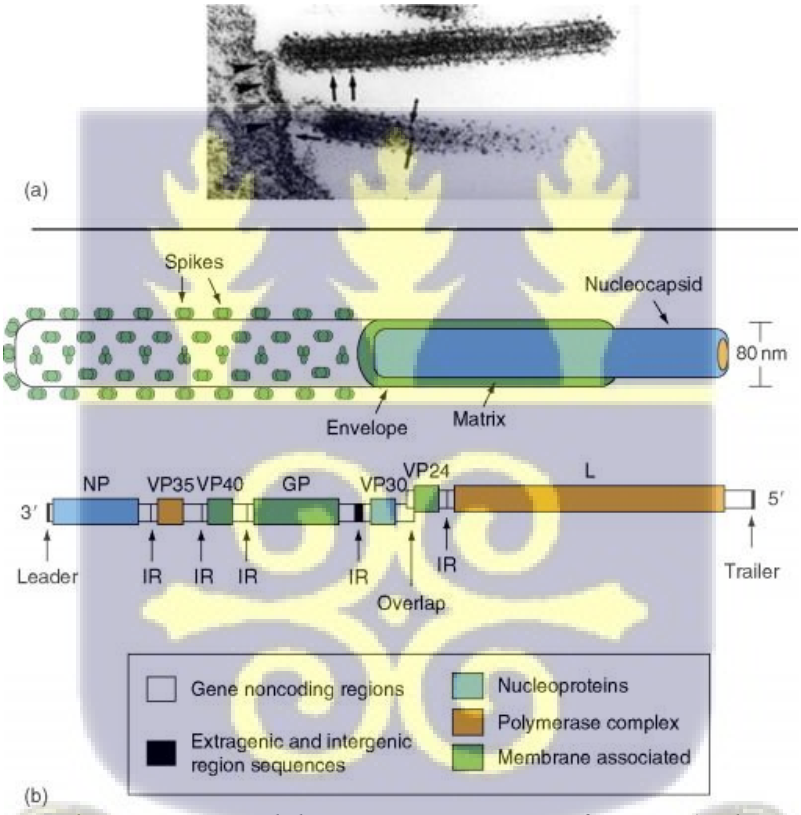

Figure 2. 4: Depicts the structure and the gene composition of MARV (Falzarano & Feldmann, 2008).

Together, SARS-CoV-2, Ebola virus, and Marburg virus represent highly pathogenic enveloped RNA viruses with devastating impacts on human health and global economies. Despite differences in genome organization and host reservoirs, they share common features: reliance on envelope glycoproteins for host cell entry, broad tissue tropism, and the capacity to

trigger severe immunopathology. Current therapeutic strategies remain limited—largely supportive in the case of filoviruses, and only partially effective antivirals and vaccines for SARS-CoV-2—underscoring the urgent need for novel interventions. Natural products, particularly secondary metabolites derived from microorganisms such as Streptomyces and Bacillus species, have historically been a rich source of antimicrobial agents and are increasingly recognized for their potential antiviral properties. By focusing on entry inhibition of these high-consequence viruses using pseudovirus models, this study directly addresses the research objectives of identifying broad-spectrum antiviral candidates. Such natural products may provide safer, more accessible options for therapeutic development and serve as a foundation for future strategies to combat emerging and re-emerging viral threats.

2.7 Natural products

Natural products remain a critical source of therapeutic agents. Microbial secondary metabolites such as polyketides, alkaloids, and flavonoids play diverse ecological roles and provide templates for drug discovery (Chin et al., 2006; Dias et al., 2012).

Bacillus species produce lipopeptides such as surfactins, iturins, and fengycins, which display antibacterial, antifungal, and antiviral activities (Barros et al., 2013; Raihan et al., 2021). Surfactins disrupt viral envelopes, while fengycins and iturins have been reported to inhibit influenza virus replication (He et al., 2021; Zhen et al., 2023). Bacillus-derived metabolites such as bacitracin remain clinically relevant antibiotics (Asif, 2014).

Streptomyces species are prolific producers of polyketides and other metabolites, including tetracyclines and actinomycin D, with known antiviral properties (Procópio et al., 2012; Yoo et al., 2015). Their genetic tractability makes them a sustainable platform for novel antiviral

discovery (Hamed et al., 2018). Recent evidence highlights Streptomyces metabolites with activity against coronaviruses and enteroviruses (Huang et al., 2021; Yu et al., 2023).

Taken together, Bacillus and Streptomyces metabolites represent a promising resource for discovering viral entry inhibitors. Screening these compounds with pseudovirus assays provides a rational strategy for identifying candidates with potential broad-spectrum activity.

CHAPTER THREE

3.0 Methods

3.1 Study design

This study was an *in vitro* experimental study which involved the production of lentivirus-based pseudoviruses for SARS-CoV-2, Marburg virus, and Ebola virus, with a subsequent evaluation of antiviral activity from natural compounds derived from *Bacillus* and *Streptomyces* species.

The compounds were isolated and purified from *Bacillus* and *Streptomyces* species collected from the Digya National Park, Bono East Region, Ghana. These compounds are from a novel strain and their structures and some bioactivity against some parasites had been recently elucidated (doi: 10.3762/bjoc.18.185). Due to confidentiality, compound structures are not disclosed here and will be identified with numeric values (Table 3.1).

Table 3. 1: Natural Product derived from Novel strains of Streptomyces sp and Bacillus sp

Bacterial Species	Compound #
Streptomyces sp. Pillar 1M stock B	1-12
Streptomyces sp. Pil 101C 1/100 D	13-21
Bacillus sp. Pillar 1NW stock D	22-32

3.2 Production of competent cells (XL-10 gold)

Glycerol stocks of the cells, XL-10 ultracompetent cells were streaked onto a Luria Berthani (LB) agar plate with 100 µg/ml of chloramphenicol for selection of the cells and grown overnight at 37°C in an incubator. The reagents (100 mM $CaCl_2$, 100 mM $MgCl_2$ and 85 nM $CaCl_2$ with glycerol) and materials to be used in this experiment were chilled overnight at 4°C. Ten milliliters of LB starting culture were inoculated with a single colony of *E. coli* that was

selected, which was shaken and kept at 37°C for the entire night. Following overnight incubation, into a 1 L of LB media, 10 mL of the starting culture was used for the inoculation and incubated at 37°C with shaking. The optical density of the cells was measured every hour at a wavelength of 600 nm and every 15 – 20 min when the optical density was above 0.2. On ice, the cells were cooled for about 25 min with intermittent swirling when the OD reached between 0.35 and 0.4. Following this, the 1 L culture was split into four equal parts and transferred to prechilled centrifuge tubes, which were then spun for 15 minutes at 3000g and 4°C. The supernatant was discarded, and the pelleted cells were combined in one centrifuge tube and resuspended in approximately 100 mL of ice-cold $MgCl_2$ solution. The cells were then spun at 2000g and a temperature of 4°C for another 15 min. Following centrifugation, the supernatant was discarded, and the resulting cell pellet was gently resuspended in approximately 200 mL of ice-cold calcium chloride ($CaCl_2$) solution. The suspension was incubated on ice for 20 minutes. Subsequently, the cells were centrifuged at 2,000 × *g* for 15 minutes at 4°C. The pellet was then resuspended in roughly 50 mL of an ice-cold solution containing 85 mM $CaCl_2$ and 15% glycerol. This suspension was transferred into a prechilled 50 mL conical tube and centrifuged again at 1,000 × *g* for 15 minutes at 4°C. The final pellet was resuspended in 2 mL of the same ice-cold $CaCl_2$ glycerol solution. Aliquots of 50 µL were dispensed into sterile 1.5 mL microcentrifuge tubes and snap-frozen in liquid nitrogen for storage. Until their next use, the frozen cells were kept at -80 °C.

3.3 Bacterial transformation

Luria-Bertani (LB) agar was prepared by dissolving 7.5 g of agar and 12.5 g of LB base powder (Sigma-Aldrich, L3022) in 500 mL of distilled water within a reagent bottle. The mixture was sterilized by autoclaving and subsequently allowed to cool. Once cooled to an appropriate

temperature, the medium was poured into sterile petri dishes under aseptic conditions near a flame to minimize contamination.

LB broth was prepared by following the manufacturer's instruction. Briefly, 12.5 g of LB powder was weighed into a reagent bottle, and 500 mL of distilled water was added. The medium was then autoclaved before use for growth of small cultures for extraction. The autoclaved broth after use was stored at 4°C.

In preparation of plates/broth cultures, Ampicillin is added to the medium at a concentration of 100 µg/mL from a stock of 100 mg/mL, that is a 1: 1000-fold dilution of the antibiotic.

Cells were transferred into 1.5 mL microcentrifuge tubes on ice. After this, 2 µL of 10 ng/µL of resuspended DNA was added to the microcentrifuge tubes containing 20 µL of competent cells. The mixtures were incubated on ice for 30 min, with gentle flicking of the tubes to mix the solution. The tubes were placed back on ice after the 30-minute incubation period and then incubated for 30 seconds at 42°C in a water bath. Following this, 100 µL of prewarmed Luria Bertani (LB) broth media was added to each reaction tube, and the tubes were incubated at 37°C while shaking at 180 rpm for 1 h. After the 1 h incubation, 25 µL of the transformed cells were transferred to pour plates and spread with a sterile spreader. Poured plates with ampicillin were used as negative controls, whereas those without ampicillin served as positive control with a known plasmid with ampicillin resistance. The inoculated plates were incubated at 37°C for approximately 16–18 hours to allow colony formation. Following incubation, individual colonies were selected, and each was transferred into 10 mL of LB broth. These cultures were then incubated at 37°C with agitation at 180 rpm for 16 hours to promote bacterial growth.

Single colonies from transformation were grown in antibiotic broth at 37℃ for 16-18 hours. After which extraction of the plasmids was performed.

3.4 Plasmid extraction

The QIAprep® Spin Miniprep Kit (QIAGEN, Hilden, Germany, catalog number: 27106) was used to extract plasmids, following the manufacturer's protocol with few modifications. Briefly, after centrifuging the culture in broth for seven minutes at 5,000 rpm, the supernatant was disposed of. In 250 µL of Buffer P1, the pellet was suspended in the resuspension buffer. he resuspended cells were transferred into labeled 1.5 mL microcentrifuge tubes. To each tube, 250 µL of Buffer P2 (lysis buffer) was added, and the contents were gently mixed by inverting the tube 4–6 times until the solution turned uniformly blue, indicating complete lysis. After 5 minutes, 350 µL of Buffer N3 (neutralization buffer) was added, and the mixture was again gently inverted 4–6 times until the solution became clear. The tubes were then centrifuged at 13,000 rpm for 10 minutes. Approximately 800 µL of the resulting supernatant was carefully transferred to a QIAprep 2.0 spin column and centrifuged at 13,000 rpm for 1 minute to bind plasmid DNA to the column membrane. The filtrate in the collection tubes is discarded, and 500 µL Buffer PB which is the binding buffer, is added to the spin column and centrifuged at 13,000 rpm for 1 min to allow the DNA to bind well and serve as a wash step. The filtrate in the collection tubes is discarded. To wash the bound plasmid DNA, 750 µL of Buffer PE (wash buffer) was added to the QIAprep 2.0 spin column, followed by centrifugation at 13,000 rpm for 1 minute. The flow-through was discarded, and the column was centrifuged again for an additional minute to remove any residual wash buffer. The spin column was then transferred to a sterile 1.5 mL microcentrifuge tube. For elution, 50 µL of Buffer EB (elution buffer) was applied directly to the center of the column membrane, incubated at room temperature for 1 minute, and subsequently centrifuged for 1 minute to elute the plasmid DNA. The concentration and purity of the extracted plasmid DNA were determined using a NanoDrop (ThermoFisher Scientific, Waltham, MA, USA). The presence of the desired plasmid was confirmed by restriction digest.

3.5 Restriction digest of plasmid

All reagents were thawed on ice. The reaction mixes of a total volume of 15 µL are placed in a 1.5 mL microfuge tube. The reagents are added in the following order: buffer, water, DNA template, and restriction enzyme(s).

1. 1.5 µL of the Fast digest buffer
2. Nuclease-free water is added based on the concentration of the DNA.
3. 10 µg/µL of plasmid (DNA)
4. 0.5 µL each of the specific restriction enzymes used.

The reaction mix was incubated at 37°C for an hour. A 1% agarose gel was prepared, and samples were run and analyzed via gel electrophoresis.

The template DNA was removed from the reaction to provide a negative control.

3.6. Cell Culture and Seeding

Human embryonic Kidney 293T cells were maintained in Dulbecco's minimum essential media (DMEM) enriched with 10% Fetal Bovine Serum (FBS) and 1% Penicillin-Streptomycin. Cells are incubated at 37℃ in the presence of 5% Carbon dioxide. Cells were subcultured weekly in a T75 flask 1 to 3.

The maintenance media of HEK293T cells in culture was aspirated. Approximately 5 mL of PBS was transferred to the cell-free side of the T-75 flask and gently swirled over the cell layer to rinse off residual media. The PBS was then aspirated. Next, 1 mL of trypsin was added to the flask and gently swirled over the cell layer. To aid in cell dissociation, the flask was incubated for approximately three minutes at 37°C with 5% CO_2. For detachment, cells were examined under a microscope. To stop trypsinization, the cells were mixed with around 5 mL of growth media that had been heated beforehand. The cell suspension was then moved to a

centrifuge tube, where it was spun for five minutes at 1000g. After centrifugation, the supernatant was discarded, and the pellet was resuspended in 2 mL of prewarmed culture medium. A 10 µL aliquot of the cell suspension was mixed with an equal volume (10 µL) of 0.4% (w/v) trypan blue dye. After gentle mixing, 10 µL of the stained cell mixture was loaded onto a LUNA-II counting slide, and cell viability was assessed using the LUNA-II Automated Cell Counter (Logos Biosystems, Annandale, VA, USA). After that, 10 cm tissue culture dishes with 10 mL of prewarmed DMEM were filled with 1.5 mL of cell suspension with 5,000,000 live cells/mL, and the dishes were incubated for the entire night at 37°C with 5% CO_2.

3.7 Optimization of Transfection methods for Pseudovirus Production (Ebola, Marburg, and SARS-CoV-2)

In brief, HEK 293T cells were co-transfected with three plasmids. The HIV gag-pol plasmid, pCMV-dR8.91, supplies the necessary structural and enzymatic components required for viral particle assembly. The luciferase reporter plasmid, pCSFLW, is important for measuring transfection efficiency and activity through luciferase assays, were kind gifts from Professor Osbourne Quaye who collaborates with Professor Edward Wright from the University of Sussex (Murray et al., 2021). Both plasmids were co-transfected with either the envelope plasmid of the virus of interest, pCAGGS EBOV Makona, pCAGGS MARV DRC G2, which were both also kind gifts from the Quaye Lab or pcDNA 3.1 SARS-CoV-2 S (Addgene, 145032) using transfection techniques defined below. Media containing the SARS-CoV-2 pseudovirus were harvested after 48 hours and 72 hours post-transfection. The same was done for the other pseudoviruses, EBOV and MARV. The pseudovirus was filtered using a 0.45 µM syringe-driven filter to remove cellular debris. Harvested viruses were aliquoted and stored at -80℃ until use. Mock pseudovirus were made by transfecting HEK 293T cells with just the HIV gag-pol plasmid pCMV-dR8.91 and luciferase reporter plasmid, pCSFLW.

3.7.1 Calcium Phosphate

Calcium phosphate precipitation transfection was carried out to allow entry of plasmids for cell line production and pseudovirus production into HEK293T cells (Chen, 2012). Briefly, the transfection reagent concentrations were prepared; 2 M CaCl2 was prepared using CaCl2 and distilled water and the solution was filtered under aseptic condition using a 0.2 µm syringe filter and stored at room temperature. The HEPES Buffered Saline (HBS) at 2X was prepared with 50 mM HEPES, 280 mM NaCl and 1.5 mM Na2HPO4. The solution was filtered, aliquoted in microcentrifuge tubes and stored at -20°C.

Briefly, 5 × 10^6 HEK293T cells were seeded into a 10 cm^2 tissue culture dish 24 hours prior to transfection and maintained at 37 °C in a humidified incubator with 5% CO_2. Approximately three hours before transfection, the culture medium was refreshed. Co-transfection of the three plasmids into HEK293T cells was performed using the calcium phosphate precipitation method, as previously described. Nuclease-free water, 5 µg of env plasmid, 3 µg of luciferase reporter plasmid (pCSFLW), 4.5 µg of Gag pol packaging system plasmid (p8.91), and 24.4 µL of 2 M CaCl2 are all present in Solution A, a 200 µL mixture. The mixture was incubated for 30 minutes at ambient temperature after Solution A was added dropwise to 200 µL of 2X HBS. The mixture was then gently stirred every 10 minutes. Three hours after the dish had been restocked with fresh medium, the resulting mixture was carefully moved and added to the cells. After 24 hours, the medium was replaced, and 48 and 72 hours after transfection, the pseudovirus in the supernatant was extracted and filtered through a 0.45um filter.

An 11-series two-fold dilution of the harvest was prepared in duplicate in a round-bottom 96-well plate to measure the PV generated. The following day, the dilutions were put onto ACE2-HEK293 cells that had been pre-seeded at 20,000 cells per well in a white 96-well plate

(catalogue no: 136101). Infected cells were maintained at 37 °C with 5% CO_2 for 24 hours post-infection. Pseudoviral titers were determined by quantifying luciferase activity, measured in relative luminescence units (RLU), using the Bright-Glo™ luciferase reagent. Plotting an RLU against dilution factor graph allowed for the selection of a working dilution at a cut-off of 1,200,000 RLU.

3.7.2 Polyethyleneimine (PEI) transfection

Two hours before transfection, the media from 5×106 HEK293 cells that were seeded overnight was replaced with pre-warmed DMEM that had been supplemented with 10% FCS. The three plasmids, pCMV-dR8.91, pCSFLW, and a plasmid that encodes the envelope glycoprotein of either SARS-CoV-2, Ebola virus, and Marburg virus were added to 200 µL of DMEM/OptiMEM in a microcentrifuge tube in the amounts of 3 µg, 5 µg, and 4.5 µg, respectively. In a separate tube, 60 µL of 1 mg/mL PEI was added to 200 µL of DMEM/OptiMEM, and both tubes were incubated at room temperature. After incubation, the PEI mixture was added to the DNA mix. The PEI-DNA mix was gently flicked across a microcentrifuge rack to mix and then cultivated for 20 minutes at room temperature. Following this, the PEI-DNA mix was added dropwise to the cells, and the plate was swirled gently to ensure distribution to other parts of the plate. The plate was kept in an incubator with 5% CO2 at 37°C. After 14 hours of incubation, the spent media was replaced with pre-warmed DMEM and incubated for 48 to 72 hours.

3.7.3 Lipofectamine transfection

Plasmid DNA transfection was performed using Lipofectamine™ 3000 (Thermo Fisher Scientific, Waltham, MA, USA) in accordance with the manufacturer's protocol. HEK293T cells were seeded at a density of 5 × 106 cells per dish, reaching approximately 70–90%

confluency at the time of transfection. Lipofectamine 3000 reagents was diluted in Opti-MEM medium. DNA samples were prepared by diluting them in an Opti-MEM medium. Diluted DNA samples were added to diluted Lipofectamine 3000 in a ratio of 1:1 and incubated at room temperature for about 10 minutes and then added to the cells. Cells were maintained at 37 °C in a humidified 5 % CO_2 atmosphere, and culture supernatants were collected at 48 h and 72 h post-incubation.

3.8 Pseudovirus activity/infectivity assay

To verify pseudovirus activity, about 100 µL of media and 50 µL PV were added to the ACE-HEK293 cells and after 24 hours, luciferase activity was determined using Promega BrightGlo reagents (Promega, E2650). This was done following the manufacturer's instructions as described below. 1 in 2 dilutions of the BrightGlo reagent was made using complete DMEM. Media was discarded from the plate and plates were blotted on a paper towel to remove excess media. 50 µL of diluted BrightGlo reagent was added to each well and after three min of incubation, the luminescence was read using a GloMax plate reader. Cells only and cells with the mock virus were used to determine the background signal.

3.9 Plasmid-Mediated hACE2 Expression in HEK293 Cells

HEK293 was transfected with the human ACE2 plasmid, pcDNA3.1-hACE2 (hACE2), using a modified calcium phosphate technique. Briefly, 3×10^5 cells were cultivated in a 10 cm dish at 37ºC with 5% CO2. The media was replaced after 24 hours and three hours before to transfection, and the cells were maintained in the same conditions. To a sterile tube, 3, 5 and 8 µg of the *hACE2* plasmid into HEK293 cells, 12.2 µL of 2M $CaCl_2$ and nuclease-free water were added to reach a total volume of 100 µL, then mixed gently. The mixture was added dropwise to another sterile tube containing 100 µL of 2x HEPES Buffered Saline (HBS) and

incubated at room temperature for 30 min. The transfection mixture was mixed at 10 min intervals by gently tapping the base of the tube. The resulting plasmid-calcium phosphate complex in solution was then added dropwise to the seeded cells. For transient expression of ACE2, cells were harvested 24 hours-post transfections and used for pseudovirus infection experiments and dot blot analysis.

3.10 Production of ACE2-HEK293 which stably expresses hACE2.

Geneticin resistance encoded *pcDNA3.1-hACE2* (Addgene, 145033**)** was used to select cells with the ability to stably express hACE2 over multiple passages. The concentration of the antibiotic (geneticin/G418) needed to eradicate all non-transfected cells in two weeks was calculated using a kill curve. In short, cells were cultured for two weeks in medium supplemented with progressively higher quantities of G418. After two weeks, trypan blue staining and a hemocytometer were used to assess cell viability under a microscope. 1000 µg/mL was selected for further use based on this. Following transfection as previously mentioned, cells were cultivated for two weeks. To select for ACE2-HEK293 cells, the media was replaced every two days with new media containing 1000 µg/mL geneticin. It is expected that non-ACE2-HEK293 cells would die within that period. The cells were eventually passaged in 100 µg/mL of geneticin after the concentration was gradually lowered to 500 µg/mL after two weeks. ACE2-HEK293 transfected steadily Before being used, the cells were kept in liquid nitrogen and frozen in freezing medium. Using a Dot blot test, the expression of ACE2 in freshly thawed cells was confirmed.

3.11 Dot blot to detect expression of ACE2 in cells after transfection.

To assess ACE2 receptor expression, ACE2-HEK293 cells were lysed using a freeze-thaw method in the presence of a protease inhibitor (SIGMA, SCLF5528). Briefly, frozen cells were

thawed at 37 °C and supplemented with 1X protease inhibitor. The cell suspension was then subjected to another freeze cycle at –80 °C for 10 minutes, followed by a second thaw at 37 °C to complete the lysis process. With the exception of the protease inhibitor spike, this cycle is carried out five times to ensure efficient lysis. On a sterile bench, the lysate (2–10 µL) was spotted on a nitrocellulose membrane and left to air dry. The membrane was blocked using 5 percent BSA in Tris (20 mM), 150 mM NaCl, and 0.1 percent (w/v) Tween® 20 detergent (TBS-T) for 30 minutes at room temperature. A 1000X dilution of rabbit polyclonal anti-hACE2 (Abcam, GR3333640-16) was then used to probe the membrane for one hour at room temperature. TBS-T was then used to wash the membrane three times for ten minutes each at room temperature. The membrane was treated with a 10,000X dilution of goat anti-rabbit IgG HRP-conjugated antibody (Abcam, GR3299244-1) for one hour at room temperature in order to detect bound ACE2. A final wash of 1X TBS at room temperature was then performed after the membrane had been cleaned three times for ten minutes each using 1X TBS-T. A 1:1 solution of hydrogen peroxide and enhanced chemiluminescence reagent (Protein biology, VB296357) was produced in accordance with manufacturer protocol and applied to the blot just prior to imaging. To visualize blots, the Amersham™ Imager 600 was utilized.

3.12 Cytotoxicity test for compounds using Alamar Blue™ reagent.

HEK293T and ACE-HEK 293 cells in culture were seeded overnight in clear 96 tissue culture-treated well plates with 2×10^4 cells per 100 µL and incubated overnight. A starting concentration of 300 µg/mL of each compound was prepared and then serially diluted two-fold in across four dilutions in 1.5 mL microcentrifuge tubes for each compound to a final volume of 800 µL per tube, with the first tubes being filled with the prepared working concentration of the compounds (concentrations; 18.75 µg/mL, 37.5 µg/mL, 75 µg/mL, 150 µg/mL, and 300 µg/mL). The media from the overnight seeded cells was aspirated and a volume of 100 µL of

the different concentrations of compounds was transferred onto the cells in triplicate, beginning with the lowest concentration of compound. Incubation of the cells took place for 48 hours at 37°C with 5% CO2 present. After 48 hours of incubation, 10 µL of Alamar Blue™ cell viability reagent was added to each well and then the cells were incubated for an additional 6 hours. After the 6-hour incubation, fluorescence was measured using a microplate reader at 560 nm emission and excitation 590 nm.

3.13 Inhibition assay to screen for antiviral compounds.

Permissive cell lines for each virus (HEK293T/ ACE2-HEK293 cells) were seeded in a 96-well tissue culture plate at 2×10^4 cells per well and incubated at 37℃ with 5% CO_2. After 24 hours of seeding, the media was changed and pre-incubated with a warm 100 µL culture medium containing one-tenth the CC 50 (generated through the dose-response curve-cytotoxicity assay) of the compounds in triplicate. A pre-treatment period of one hour was followed by the addition of 30 µL of pseudovirus to achieve an infectivity of approximately 1×106 RLU. After 24 hours of incubation at 37 oC with 5% CO2, the Bright Glo reagent (Promega and E2650) was used to measure the luciferase activity, which indicates pseudoviral infectivity, in accordance with the manufacturer's instructions. With the GloMax® Discover Microplate Reader (Promega-GM3000), luminosity was measured.

3.14 Statistical analysis

GraphPad Prism was used for data analysis (version 9.0). A one-way ANOVA test was performed to determine if there were significant differences in the transfection efficiencies between the groups using different transfection methods. Also, pairwise comparisons between specific groups were conducted using t-tests to analyze further which methods differed in efficiency. Values were presented as *p < 0.0332, **p < 0.0021, ***p < 0.0002, ****p <

0.0001. Error bars are standard errors of the mean. All statistical details of experiments can be found in the figure legends.

4.0. RESULTS

4.1 Stable and Transient Expressing ACE2 HEK293 Cells are Highly Efficient for SARS-CoV-2 infection

The role of the ACE2 receptor in facilitating SARS-CoV-2 pseudovirus entry into HEK293 cells was evaluated. Transient transfection with ACE2 plasmid at concentrations of 3 µg, 5 µg, and 8 µg resulted in significantly higher pseudoviral infectivity compared with untransfected controls, with a clear dose-dependent enhancement of entry (Figure 4.1A).

Transient receptor expression was confirmed one-week post-transfection by dot blot analysis, which detected ACE2 protein bands in transfected cells but not in untransfected controls (Figure 4.2B). For stable expression, cells were subjected to geneticin (G418) selection. Dot blot analysis of lysates collected at four- and six-weeks post-selection demonstrated sustained ACE2 expression, with markedly higher levels at six weeks compared with four (Figure 4.2C). Constitutive ACE2 expression was also detected in both the supernatant and pellet fractions, likely reflecting release during lysis. These findings confirm the successful establishment of a stable ACE2-HEK293 cell line with consistent receptor expression suitable for SARS-CoV-2 pseudovirus assays.

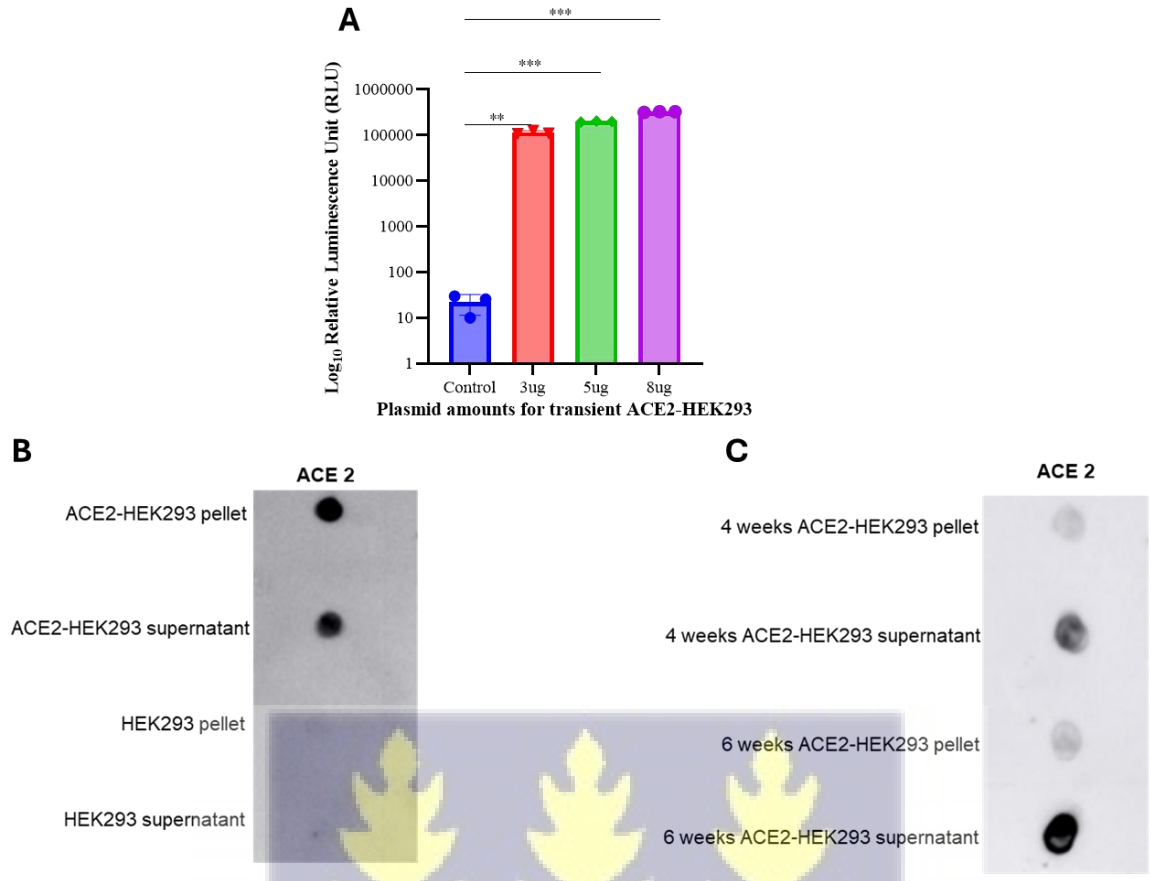

Figure 4. 1: Development and validation of ACE2-HEK293 cell line for SARS-CoV-2 pseudovirus infection. (A) The optimisation of pseudovirus entry was assessed by transfecting HEK293 cells with increasing concentrations of ACE2 plasmid (3 µg, 5 µg, and 8 µg), which showed a dose-dependent increase in infectivity compared to untransfected controls (n=3). (B and C) Dot blot analysis confirming ACE2 receptor expression. Transient expression (B) was detected one week post-transfection, while stable expression (C) was demonstrated in both pellet and supernatant fractions after 4 and 6 weeks of G418 selection, with higher levels observed at the six-week time point. (**p < 0.0021, ***p < 0.0002).

4.2 Verification of Plasmid Integrity for Pseudovirus Production

The extracted plasmids were subjected to restriction enzyme digestion to verify their identity and integrity. Specific restriction enzymes were selected based on the plasmid maps. The plasmids were digested using a list of enzymes shown in Table 4.1 below with the band sizes as listed. Shown (Figure 4.2) is a 1% Agarose gel electrophoresis of the digested plasmids for pseudovirus production; the HIV gag-pol plasmid (pCMV-dR8.91), luciferase reporter plasmid (pCSFLW) the envelope plasmids of the virus of interest (pcDNA 3.1 SARS-CoV-2 S (cat no: 145032) or pCAGGS EBOV Makona or pCAGGS MARV DRC G2). The DNA was

successfully digested using different restriction enzymes at the required restriction sites (table 4.1). Different band sizes were visible on the gel electrophoresis (figure 4.2), and they matched the predicted sizes of the target DNA fragments.

Table 4. 1: Plasmids were digested with the specific restriction enzymes and the expected band sizes.

Plasmids	Restriction enzyme	Band
SARS-CoV-2 (D614G)	Nhe1 + Xho1	6.5kb and 5.2kb
pCAGGS EBOV Makona	Kpn1 + Xho1	4.8kb and 2kb
pCAGGS ZEBOV Mayinga	Kpn1 + Xho1	4.8kb and 2kb
pCAGGS MARV DRC G2	EcoR1 + Nhe1	4.8kb and 2kb
pCMV-dR8.91	Bgl111	8.2kb and 3.9kb
pCSFLW	BamH1 + Not1	8.9kb and 1.7kb

Figure 4. 2: Electropherogram of digested plasmids. Restriction digest product was run on a 1% agarose gel to detect plasmids for pseudovirus production. The digested plasmids resolved on an agarose gel are shown. Samples containing 10 µg plasmids treated with restriction enzymes in Table 4.1 and separated on the agarose gel with Ethidium Bromide for 1 h. A 1kb molecular weight ladder was used.

4.3 Different Methods of Transfection Gives Different Efficient in Pseudovirus Production

To optimize pseudovirus generation, three distinct transfection reagents—lipofectamine, polyethyleneimine (PEI), and calcium phosphate—were evaluated for their ability to produce pseudoviruses bearing the envelope glycoproteins of Ebola virus (EBOV-Makona), SARS-CoV-2, and Marburg virus (MARV). The efficiency of each method was assessed by quantifying pseudovirus infectivity in HEK293T or ACE2-HEK293 cells using a luciferase-based readout.

For EBOV-Makona pseudoviruses, all three transfection methods yielded infectious pseudoviruses; however, lipofectamine and calcium phosphate demonstrated superior efficiency compared to PEI. To determine the optimal harvest time, pseudovirus-containing supernatants were collected at 48- and 72-hours post-transfection. Across all methods, higher pseudovirus yields were observed at the 48-hour time point, indicating that earlier harvest improved pseudovirus recovery and infectivity. These results identify lipofectamine and calcium phosphate as robust methods for EBOV pseudovirus generation, with 48 hours post-transfection representing the optimal harvest window.

In the case of SARS-CoV-2 pseudoviruses, lipofectamine transfection resulted in significantly higher pseudovirus production compared with calcium phosphate, as measured by infectivity in ACE2-expressing cells. PEI transfection did not yield detectable SARS-CoV-2 pseudoviruses under the tested conditions, suggesting that this method was unsuitable for efficient pseudovirus production. These findings underscore the importance of reagent selection, with lipofectamine identified as the most reliable method for generating SARS-CoV-2 pseudoviruses for downstream entry and neutralization assays.

For MARV pseudoviruses, PEI transfection outperformed calcium phosphate, producing substantially higher titres and infectivity. Lipofectamine transfection was attempted but did not result in measurable pseudovirus generation, highlighting virus-specific variability in transfection efficiency. The superior performance of PEI for MARV indicates that optimization of transfection conditions must be tailored to individual viral glycoproteins to achieve maximal pseudovirus production.

Collectively, these results demonstrate that transfection efficiency varies across viral pseudotypes and reagents. Lipofectamine was optimal for SARS-CoV-2, calcium phosphate and lipofectamine were most effective for EBOV, while PEI was the most successful for MARV. These findings establish a virus-specific framework for pseudovirus generation, ensuring reliable production of high-titre pseudoviruses for use in antiviral screening assays.

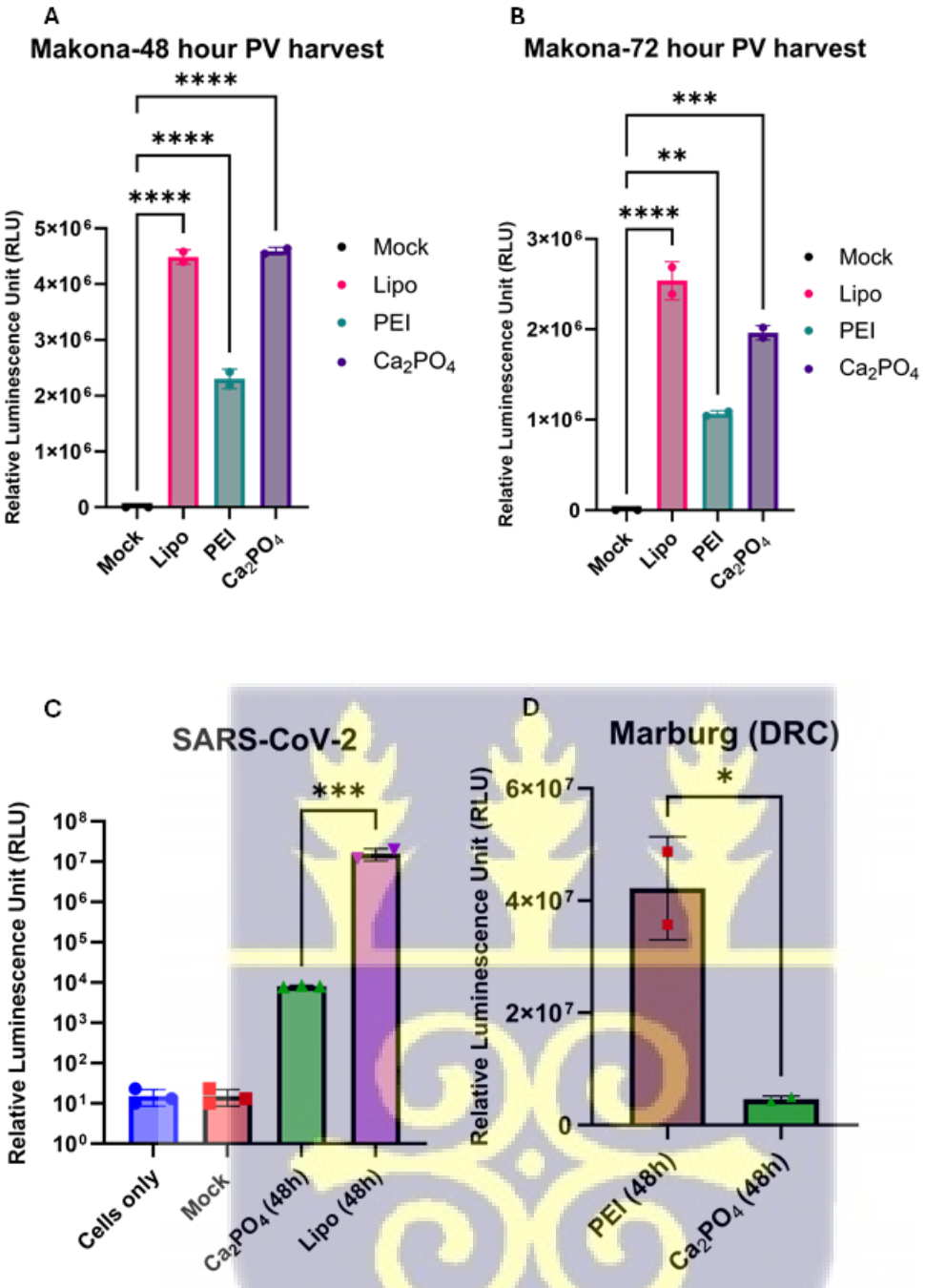

Figure 4. 3: Optimization of pseudovirus production using different transfection methods. (A and B) EBOV-Makona pseudoviruses were generated using lipofectamine, PEI, or calcium phosphate and harvested at 48- or 72-hours post-transfection. (C) SARS-CoV-2 pseudoviruses were produced using lipofectamine and calcium phosphate, with lipofectamine yielding significantly higher titres; Infectivity was measured in ACE2-HEK293 cells, with cell-only and mock controls included. (D) MARV pseudoviruses were generated using PEI and calcium phosphate, with PEI producing substantially higher pseudovirus titres, with no mock sample which shows very low background signals in A, B and C. Data are presented as means of biological replicates (A, B and D has n = 2 and C is n=3). Statistical significance is indicated as *p < 0.0332, **p < 0.0021, ***p < 0.0002, ****p < 0.0001.

4.4 Cytotoxicity Profiling of Compounds in HEK293T and ACE2-HEK293 Cells

The cytotoxic effects of 32 compounds were assessed in HEK293T cells using the Alamar Blue assay. Dose–response experiments across five concentrations (18.75 µg/mL, 37.5 µg/mL, 75 µg/mL, 150 µg/mL, and 300 µg/mL) demonstrated that most compounds exhibited dose-dependent cytotoxicity. However, compounds 9, 10, 20, and 22 showed little to no cytotoxicity even at the highest tested concentrations (150–300 µg/mL), indicating a more favourable safety profile (Figure 4.4). CC_{50} values were derived from nonlinear regression analysis, providing a comparative measure of compound toxicity. Data represent the mean of three technical replicates from two independent biological experiments (appendix 1).

In ACE2-HEK293 cells, all compounds exhibited minimal cytotoxicity at 100 µg/mL, with most maintaining cell viabilities close to 100% (Figure 4.3B). These results indicate that while some compounds display cytotoxic effects at higher doses in HEK293T cells, all compounds were well tolerated at a physiologically relevant concentration in ACE2-expressing cells, supporting their suitability for antiviral screening.

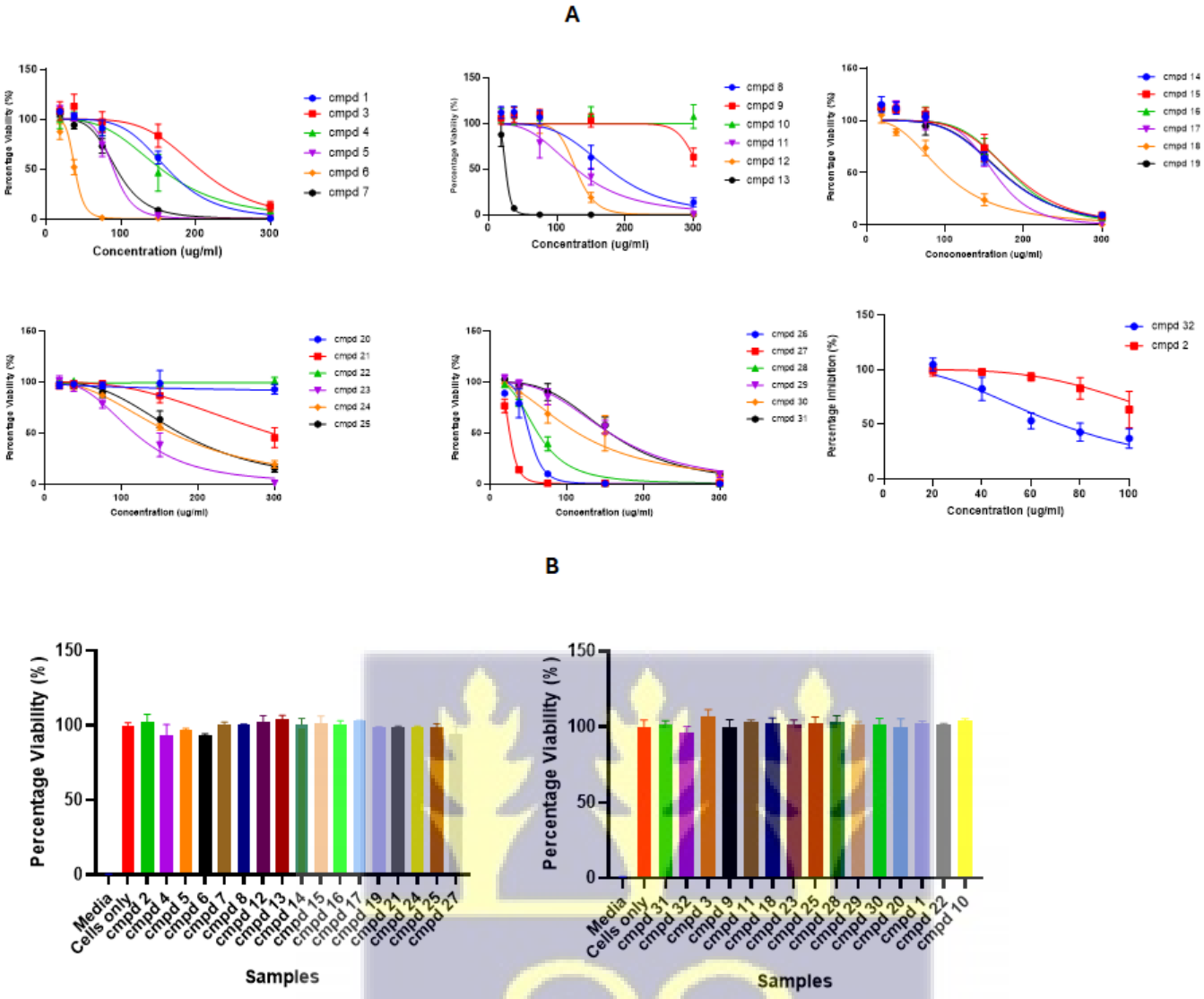

Figure 4. 4: Cytotoxicity profiling of compounds in HEK293T and ACE2-HEK293 cells. (A) Dose–response curves showing cytotoxicity of compounds (1–32) in HEK293T cells at concentrations ranging from 18.75 to 300 µg/mL. Compounds 9, 10, 20, and 22 exhibited little or no cytotoxicity even at higher concentrations. CC_{50} values were derived by nonlinear regression analysis. (B) Cytotoxicity of the same compounds in ACE2-HEK293 cells at 100 µg/mL. All compounds showed minimal cytotoxicity, with most maintaining >95% viability. Data represent the mean of three technical replicates from two independent biological experiments.

4.5 Antiviral Activity of Compounds Against Pseudoviruses

The inhibitory potential of the 32 test compounds was evaluated against MARV, SARS-CoV-2, and EBOV pseudoviruses in cell-based assays. The objective was to identify compounds capable of significantly reducing viral entry and infection. Compounds achieving less than 20%

residual infectivity were classified as highly inhibitory, corresponding to ≥80% reduction in pseudoviral infection relative to untreated controls. Cells exposed only to pseudoviruses without compounds served as infection controls.

Among the 32 compounds tested, compounds 28 and 30 demonstrated strong inhibitory activity against MARV pseudovirus, reducing infectivity below the 20% threshold. The remaining compounds displayed varying levels of inhibition but did not meet the defined cut-off, with several showing minimal or no activity (Figure 4.5). These findings highlight compounds 28 and 30 as the most promising candidates for further evaluation against MARV. (figure 4.5).

Screening against EBOV pseudovirus identified five compounds (23, 24, 29, 30, and 31) with infectivity levels below the 20% threshold, indicating potent inhibitory activity. The majority of compounds displayed only partial inhibition, while some had negligible effects. These findings highlight compounds 23, 24, 29, 30, and 31 as strong candidates for further evaluation in EBOV-targeted antiviral development (Figure 4.5B).

Seven compounds (2, 4, 5, 6, 13, 16, and 27) demonstrated high inhibitory activity against SARS-CoV-2 pseudovirus, with infectivity reduced to below the 20% threshold. The remaining compounds exhibited moderate to low inhibition or none at all. These results identify multiple promising candidates for further development as inhibitors of SARS-CoV-2 entry (Figure 4.5C).

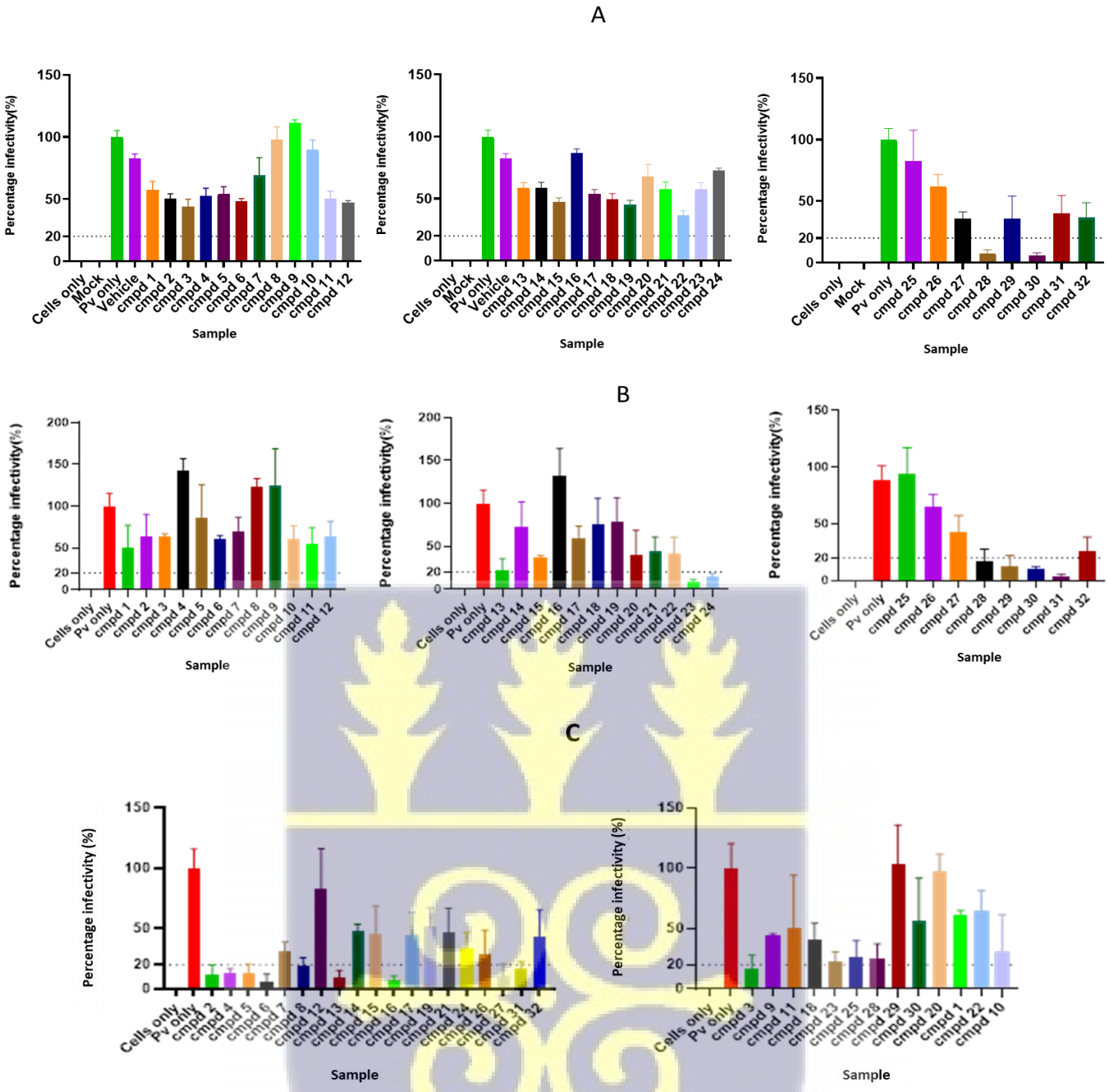

Figure 4. 5: Inhibition assays of compounds against pseudoviruses. (A) MARV pseudovirus infectivity was strongly inhibited by compounds 28 and 30. (B) EBOV pseudovirus infectivity was significantly reduced by compounds 23, 24, 29, 30, and 31. (C) SARS-CoV-2 pseudovirus infectivity was reduced below the 20% threshold by compounds 2, 4, 5, 6, 13, 16, and 27. Compounds were classified as highly inhibitory when infectivity was reduced to <20% compared with untreated pseudovirus-infected controls. Data represent three independent replicates with two biological repeats.

CHAPTER FIVE

5.0 Discussion

The present study successfully established pseudovirus-based systems for SARS-CoV-2, Ebola virus (EBOV), and Marburg virus (MARV), providing a safe and versatile platform for studying viral entry and screening antiviral compounds under BSL-2 conditions. Several important findings emerged, each of which carries implications for future therapeutic development.

The generation of both transient and stable ACE2-expressing HEK293 cell lines confirmed the critical role of ACE2 in mediating SARS-CoV-2 entry. Higher concentrations of ACE2 plasmid correlated with a dose-dependent increase in pseudovirus infectivity, consistent with previous studies highlighting ACE2 as the primary receptor for SARS-CoV-2 (Hoffmann et al., 2020; Shang et al., 2020). The successful development of a stable ACE2-HEK293 cell line provides a reliable and reproducible tool for subsequent infection and inhibition assays. Such engineered lines have been instrumental in coronavirus research, as they allow for consistent viral entry studies and can be cryopreserved for long-term use without loss of functionality (Nie et al., 2020).

Furthermore, pseudovirus production efficiency varied across different transfection methods and viral glycoproteins. For EBOV, calcium phosphate and lipofectamine were the most effective transfection methods, with optimal pseudovirus yield at 48 hours post-transfection. This finding aligns with previous reports demonstrating that earlier harvest times improve pseudovirus infectivity by preserving glycoprotein stability (Whitt, 2010). For SARS-CoV-2, lipofectamine-mediated transfection was markedly more efficient than calcium phosphate, while PEI failed to produce infectious pseudoviruses under the tested conditions. Interestingly, MARV pseudoviruses were most efficiently generated using PEI, while lipofectamine was ineffective. This highlights the virus-specific requirements for pseudovirus assembly and

suggests that transfection efficiency is influenced by glycoprotein compatibility with the chosen vector system, as observed in other filovirus pseudotyping studies (Takada et al., 1997; Ou et al., 2020).

Additionally, the cytotoxicity profiling of 32 compounds revealed that most of the compounds showed a dose-dependent toxicity in HEK293T cells, while compounds 9, 10, 20, and 22 exhibited little or no cytotoxicity even at the highest concentrations tested. Importantly, all compounds maintained high viability in ACE2-HEK293 cells at 100 µg/mL, indicating that the selected working concentrations were suitable for antiviral screening. These findings underscore the necessity of cytotoxicity assays in early drug discovery to distinguish specific antiviral effects from non-specific cellular toxicity (Xia et al., 2018).

The inhibition assays revealed several promising antiviral candidates. For EBOV, five compounds (23, 24, 29, 30, and 31) exhibited strong inhibitory activity, reducing infectivity by ≥80%. For MARV, only compounds 28 and 30 achieved similar levels of inhibition. Notably, compound 30 inhibited both EBOV and MARV, suggesting potential as a broad-spectrum anti-filovirus entry inhibitor. Previous studies have emphasized the challenge of identifying cross-reactive inhibitors due to structural differences in filovirus glycoproteins (Côté et al., 2011), making this observation particularly significant. For SARS-CoV-2, seven compounds (2, 4, 5, 6, 13, 16, and 27) displayed potent inhibition, consistent with recent reports of natural product-derived inhibitors targeting the spike–ACE2 interaction (Hoffmann et al., 2020; Wu et al., 2022).

These results highlight the utility of pseudovirus-based assays as a robust platform for antiviral screening. The identification of compounds with selective activity against SARS-CoV-2, EBOV, and MARV provides a foundation for further mechanistic studies and medicinal chemistry optimization. Particularly, the discovery of compound 30 as a dual EBOV/MARV

inhibitor is promising, as pan-filovirus antivirals remain an unmet need in global health preparedness (Cross et al., 2016).

Future work should include mechanistic investigations to determine whether these compounds directly block glycoprotein–receptor interactions, interfere with membrane fusion, or act on host factors involved in viral entry. Additionally, confirmatory assays using authentic viruses in BSL-3/4 facilities will be essential to validate the pseudovirus findings. The potential for structural optimization of lead compounds, combined with *in vivo* efficacy testing, could accelerate the development of broad-spectrum antivirals against emerging viral threats.

In summary, this study established efficient pseudovirus systems for SARS-CoV-2, EBOV, and MARV, identified several natural product-derived inhibitors with strong antiviral potential, and highlighted compound 30 as a candidate for further development as a broad-spectrum filovirus inhibitor. These findings not only contribute to the understanding of viral entry processes but also advance the search for novel antiviral therapeutics against high-consequence pathogens.

5.1 Conclusion

This study successfully established an ACE2-expressing HEK293 cell line that was highly permissive to SARS-CoV-2 pseudovirus infection, providing a robust platform for evaluating viral entry mechanisms and screening antiviral compounds. Using a lentiviral vector-based pseudovirus system, envelope glycoproteins from EBOV, SARS-CoV-2, and MARV were effectively incorporated, enabling safe and efficient production of pseudoviruses for functional assays. Screening of 32 natural product-derived compounds revealed several with significant inhibitory activity, with compound 30 demonstrating cross-filovirus inhibition against both EBOV and MARV, highlighting its potential as a broad-spectrum entry inhibitor. Collectively,

these findings establish a reliable pseudovirus assay for high-throughput antiviral screening and identify promising lead candidates for further preclinical development.

5.2 Limitations of Study

- Animal studies are necessary to evaluate the in vivo toxicity, effectiveness, and pharmacokinetics of the compounds that exhibit action, and live viral research is necessary to assess the compound's effect against pseudoviruses.
- Furthermore, it would be supportive to test the efficacy of some compounds in inhibiting viral infection of other strains of the viruses.

5.3 Recommendations

- Investigation of the pseudoviruses on other permissive cell lines to see the effect of the compounds on the viral infection.
- Compounds that showed active inhibitory activity should be screened against the pseudoviruses in a dose dependent way to determine IC_{50} values.
- There is a need to evaluate the effect of the compounds with some inhibitory activity against the live virus.

REFERENCES

Asif, M. (2014). A brief review on Bacitracin: A polypeptide antibiotic. *International Journal of Research in Pharmacy and Chemistry, 4*(3), 601–607.

Ayon, N. J. (2023). High throughput screening (HTS) in drug discovery: A review. *Pharmaceuticals, 16*(5), 690. https://doi.org/10.3390/ph16050690

Baize, S., Pannetier, D., Oestereich, L., Rieger, T., Koivogui, L., Magassouba, N., ... & Günther, S. (2014). Emergence of Zaire Ebola virus disease in Guinea. *New England Journal of Medicine, 371*(15), 1418–1425. https://doi.org/10.1056/NEJMoa1404505

Barros, J., Lemos, M. F. L., Figueiredo, J., Pinto, E., Sanches, J. F., & Vasconcelos, V. (2013). Bacillus lipopeptides as antifungal agents: Natural products for the control of mycotoxigenic fungi. *Food Control, 34*(2), 454–463. https://doi.org/10.1016/j.foodcont.2013.05.003

Blanco-Melo, D., Nilsson-Payant, B. E., Liu, W. C., Uhl, S., Hoagland, D., Møller, R., ... & tenOever, B. R. (2020). Imbalanced host response to SARS-CoV-2 drives development of COVID-19. *Cell, 181*(5), 1036–1045.e9. https://doi.org/10.1016/j.cell.2020.04.026

Borchert, M., Mulangu, S., Swanepoel, R., Tshomba, A., Afounde, A., Kulidri, A., ... & Van Der Stuyft, P. (2007). Serosurvey on household contacts of Marburg hemorrhagic fever patients. *Emerging Infectious Diseases, 13*(7), 1213–1218. https://doi.org/10.3201/eid1307.070078

Chan, J. F.-W., Kok, K. H., Zhu, Z., Chu, H., To, K. K.-W., Yuan, S., & Yuen, K.-Y. (2020). Genomic characterization of the 2019 novel human-pathogenic coronavirus isolated from a patient with atypical pneumonia after visiting Wuhan. *Emerging Microbes & Infections, 9*(1), 221–236. https://doi.org/10.1080/22221751.2020.1719902

Chen, C. (2012). Calcium phosphate transfection of eukaryotic cells. *Nature Protocols, 7*(7), 1174–1181. https://doi.org/10.1038/nprot.2012.047

Chen, J., & Guo, Y. (2015). Ebola virus: Molecular mechanisms of pathogenesis and antiviral development. *Antiviral Research, 118*, 58–68. https://doi.org/10.1016/j.antiviral.2015.03.016

Chen, R. E., Zhang, X., Case, J. B., Winkler, E. S., Liu, Y., VanBlargan, L. A., ... & Diamond, M. S. (2017). Resistance of SARS-CoV-2 variants to neutralization by monoclonal and serum-derived polyclonal antibodies. *Nature Medicine, 27*(4), 717–726. https://doi.org/10.1038/s41591-021-01294-w

Chin, Y. W., Balunas, M. J., Chai, H. B., & Kinghorn, A. D. (2006). Drug discovery from natural sources. *AAPS Journal, 8*(2), E239–E253. https://doi.org/10.1208/aapsj0802022

Cosset, F. L., & Lavillette, D. (2011). Cell entry of enveloped viruses. *Advances in Genetics, 73*, 121–183. https://doi.org/10.1016/B978-0-12-380860-8.00004-5

Côté, M., Misasi, J., Ren, T., Bruchez, A., Lee, K., Filone, C. M., ... & Cunningham, J. (2011). Small molecule inhibitors reveal Niemann–Pick C1 is essential for Ebola virus infection. *Nature, 477*(7364), 344–348. https://doi.org/10.1038/nature10380

Cross, R. W., Mire, C. E., Feldmann, H., & Geisbert, T. W. (2016). Post-exposure treatments for Ebola and Marburg virus infections. *Nature Reviews Drug Discovery, 15*(6), 423–434. https://doi.org/10.1038/nrd.2015.35

De Clercq, E. (2006). Antiviral agents active against influenza A viruses. *Nature Reviews Drug Discovery, 5*(12), 1015–1025. https://doi.org/10.1038/nrd2175

Dias, D. A., Urban, S., & Roessner, U. (2012). A historical overview of natural products in drug discovery. *Metabolites, 2*(2), 303–336. https://doi.org/10.3390/metabo2020303

Etzion, Y., & Muslin, A. J. (2009). Phenotypic screening in cardiovascular drug discovery. *Circulation Research, 104*(6), 746–749. https://doi.org/10.1161/CIRCRESAHA.109.194076

Falzarano, D., & Feldmann, H. (2008). Marburg virus. *Current Topics in Microbiology and Immunology, 329*, 93–111. https://doi.org/10.1007/978-3-540-69366-1_6

Feldmann, H., & Geisbert, T. W. (2011). Ebola haemorrhagic fever. *The Lancet, 377*(9768), 849–862. https://doi.org/10.1016/S0140-6736(10)60667-8

Frediansyah, A., Tiwari, R., Sharun, K., Dhama, K., Harapan, H., & Singh, R. K. (2022). Antiviral agents: Past, present, and future. *Frontiers in Microbiology, 13*, 835. https://doi.org/10.3389/fmicb.2022.835730

Furuta, Y., Gowen, B. B., Takahashi, K., Shiraki, K., Smee, D. F., & Barnard, D. L. (2013). Favipiravir (T-705), a broad spectrum inhibitor of viral RNA polymerase. *Proceedings of the Japan Academy, Series B, 89*(7), 285–299. https://doi.org/10.2183/pjab.89.285

Geisbert, T. W., Hensley, L. E., Larsen, T., Young, H. A., Reed, D. S., Geisbert, J. B., ... & Jahrling, P. B. (2003). Pathogenesis of Ebola hemorrhagic fever in cynomolgus macaques. *The American Journal of Pathology, 163*(6), 2347–2370. https://doi.org/10.1016/S0002-9440(10)63591-2

Geraghty, R. J., Aliota, M. T., & Bonnac, L. F. (2021). Broad-spectrum antiviral strategies and nucleoside analogs. *Viruses, 13*(4), 667. https://doi.org/10.3390/v13040667

Ghannoum, M. A., & Rice, L. B. (1999). Antifungal agents: Mode of action, mechanisms of resistance, and correlation of these mechanisms with bacterial resistance. *Clinical Microbiology Reviews, 12*(4), 501–517. https://doi.org/10.1128/CMR.12.4.501

Gordon, C. J., Tchesnokov, E. P., Woolner, E., Perry, J. K., Feng, J. Y., Porter, D. P., & Götte, M. (2020). Remdesivir is a direct-acting antiviral that inhibits RNA-dependent RNA polymerase from severe acute respiratory syndrome coronavirus 2 with high potency. *Journal of Biological Chemistry, 295*(20), 6785–6797. https://doi.org/10.1074/jbc.RA120.013679

Haim, H., Salas, I., Sodroski, J., & Harris, R. (2009). Generation of pseudoviruses with different neutralization properties. *Journal of Virology, 83*(18), 9386–9398. https://doi.org/10.1128/JVI.00571-09

Hamed, R. B., Gómez-Coca, R. B., Serra, I., & Allemann, R. K. (2018). Harnessing microbial biosynthetic potential for natural product discovery. *Current Opinion in Chemical Biology, 47*, 8–16. https://doi.org/10.1016/j.cbpa.2018.08.003

Harrison, S. C. (2015). Viral membrane fusion. *Virology, 479–480*, 498–507. https://doi.org/10.1016/j.virol.2015.03.043

He, Y., Cao, X., Jia, H., Pan, D., Li, F., Wang, W., ... & Xu, X. (2021). Antiviral activity of Bacillus-derived lipopeptides against influenza virus infection. *Frontiers in Microbiology, 12*, 618098. https://doi.org/10.3389/fmicb.2021.618098

Hoenen, T., Groseth, A., & Feldmann, H. (2019). Ebola virus: Unraveling pathogenesis to combat a deadly disease. *Trends in Molecular Medicine, 25*(3), 187–200. https://doi.org/10.1016/j.molmed.2018.12.003

Hoffmann, M., Kleine-Weber, H., Schroeder, S., Krüger, N., Herrler, T., Erichsen, S., ... & Pöhlmann, S. (2020). SARS-CoV-2 cell entry depends on ACE2 and TMPRSS2 and is blocked by a clinically proven protease inhibitor. *Cell, 181*(2), 271–280.e8. https://doi.org/10.1016/j.cell.2020.02.052

Hu, J., Gao, Q., He, C., Huang, A., Tang, N., & Wang, K. (2020). Development of a SARS-CoV-2 pseudovirus neutralization assay with a high-titer lentiviral pseudovirus. *Emerging Microbes & Infections, 9*(1), 1267–1274. https://doi.org/10.1080/22221751.2020.1772678

Huang, L., Chen, J., Cao, P., Pan, W., & Zhang, T. (2021). Natural products as sources of anti-coronavirus agents: Recent progress. *Journal of Infection and Public Health, 14*(6), 669–675. https://doi.org/10.1016/j.jiph.2020.12.016

Islam, M. T., Shafique, I., Rahman, M. M., Hannan, M. A., Rahman, M. A., & Sultana, N. (2023). Outbreaks of Marburg virus disease: A global health concern. *Pathogens, 12*(3), 415. https://doi.org/10.3390/pathogens12030415

Jackson, C. B., Farzan, M., Chen, B., & Choe, H. (2022). Mechanisms of SARS-CoV-2 entry into cells. *Nature Reviews Molecular Cell Biology, 23*(1), 3–20. https://doi.org/10.1038/s41580-021-00418-x

Kajihara, M., & Takada, A. (2015). Entry and replication mechanisms of filoviruses. *Microbiology and Immunology, 59*(4), 151–160. https://doi.org/10.1111/1348-0421.12237

Kortepeter, M. G., Bausch, D. G., & Bray, M. (2020). Basic clinical and laboratory features of filoviral hemorrhagic fever. *Journal of Infectious Diseases, 212*(Suppl 2), S204–S217. https://doi.org/10.1093/infdis/jiv351

Krishnamurthy, S., Grimshaw, A., Axson, J., Choe, S., & Miller, J. H. (2022). Drug repurposing: Current and future directions. *Journal of Translational Medicine, 20*(1), 243. https://doi.org/10.1186/s12967-022-03469-7

Lin, C. J., Lin, H. J., Chen, T. H., Hsu, Y. A., & Huang, S. H. (2021). Flavonoids as potential antiviral agents against coronaviruses. *International Journal of Molecular Sciences, 22*(19), 10432. https://doi.org/10.3390/ijms221910432

Liu, J., Cao, R., Xu, M., Wang, X., Zhang, H., Hu, H., ... & Wang, M. (2020). Hydroxychloroquine, a less toxic derivative of chloroquine, is effective in inhibiting SARS-CoV-2 infection in vitro. *Cell Discovery, 6*, 16. https://doi.org/10.1038/s41421-020-0156-0

Lu, R., Zhao, X., Li, J., Niu, P., Yang, B., Wu, H., ... & Tan, W. (2020). Genomic characterization and epidemiology of 2019 novel coronavirus: Implications for virus origins and receptor binding. *The Lancet, 395*(10224), 565–574. https://doi.org/10.1016/S0140-6736(20)30251-8

Malvy, D., McElroy, A. K., de Clerck, H., Günther, S., & van Griensven, J. (2019). Ebola virus disease. *The Lancet, 393*(10174), 936–948. https://doi.org/10.1016/S0140-6736(18)33132-5

Mangalmurti, N., & Hunter, C. A. (2020). Cytokine storms: Understanding COVID-19. *Immunity, 53*(1), 19–25. https://doi.org/10.1016/j.immuni.2020.06.017

Martinez, M. A. (2022). Compounds with therapeutic potential against novel respiratory viruses: Beyond COVID-19. *Viruses, 14*(2), 289. https://doi.org/10.3390/v14020289

Martini, G. A. (1971). Marburg agent disease: Clinical syndrome. *Marburg Virus Disease, 1*, 1–9.

Naqvi, A. A. T., Fatima, K., Mohammad, T., Fatima, U., Singh, I. K., Singh, A., ... & Hassan, M. I. (2020). Insights into SARS-CoV-2 genome, structure, evolution, pathogenesis, and therapies: Structural genomics approach. *Biochimica et Biophysica Acta (BBA) - Molecular Basis of Disease, 1866*(10), 165878. https://doi.org/10.1016/j.bbadis.2020.165878

Navaratnarajah, C. K., Warrier, R., & Kuhn, R. J. (2008). Structural basis for membrane anchoring and fusion regulation of rubella virus glycoproteins. *Proceedings of the National Academy of Sciences, 105*(15), 5703–5708. https://doi.org/10.1073/pnas.0801362105

Nie, J., Li, Q., Wu, J., Zhao, C., Hao, H., Liu, H., ... & Wang, Y. (2020). Establishment and validation of a pseudovirus neutralization assay for SARS-CoV-2. *Emerging Microbes & Infections, 9*(1), 680–686. https://doi.org/10.1080/22221751.2020.1743767

Ning, Y. J., Thiele, S., Steinke, S., Stoecker, K., Sliva, K., ... & Schwegmann-Wessels, C. (2017). Involvement of NPC1 in the entry of Ebola virus into the cell. *Nature, 477*(7364), 341–345.

Oliveira, T. C., Silva, F. A., Maia, E. H. B., Silva, L. B., & Taranto, A. G. (2023). In silico approaches in antiviral drug discovery: Advances and perspectives. *Pharmaceuticals, 16*(4), 537. https://doi.org/10.3390/ph16040537

Ou, X., Liu, Y., Lei, X., Li, P., Mi, D., Ren, L., ... & Qian, Z. (2020). Characterization of spike glycoprotein of SARS-CoV-2 on virus entry and its immune cross-reactivity with SARS-CoV. *Nature Communications, 11*(1), 1620. https://doi.org/10.1038/s41467-020-15562-9

Pattnaik, A., & Chakraborty, S. (2020). Broad-spectrum antivirals: The current landscape. *Viruses, 12*(5), 539. https://doi.org/10.3390/v12050539

Procópio, R. E., da Silva, I. R., Martins, M. K., Azevedo, J. L., & de Araújo, J. M. (2012). Antibiotics produced by Streptomyces. *Brazilian Journal of Infectious Diseases, 16*(5), 466–471. https://doi.org/10.1016/j.bjid.2012.08.014

Raihan, T., Hossain, M. I., Rahman, M. M., Islam, M. A., & Islam, M. S. (2021). Bacillus lipopeptides as antimicrobial agents: A review. *Microbial Pathogenesis, 152*, 104660. https://doi.org/10.1016/j.micpath.2021.104660

Rietdijk, W. J., Hol, E. M., & van Zanten, M. J. (2021). Phenotypic drug screening in neuroscience: Recent advances and future perspectives. *Frontiers in Pharmacology, 12*, 665. https://doi.org/10.3389/fphar.2021.665795

Rudometova, N. V., Shcherbakova, N. S., Vlasov, A. A., & Tarasova, O. A. (2022). Development of SARS-CoV-2 pseudovirus for neutralization assays. *Journal of Virological Methods, 299*, 114329. https://doi.org/10.1016/j.jviromet.2021.114329

Ryu, W. S., Kim, C. H., & Lee, J. H. (2021). Viral strategies of non-enveloped viruses to escape host immunity. *Virology Journal, 18*(1), 190. https://doi.org/10.1186/s12985-021-01670-y

Shang, J., Wan, Y., Luo, C., Ye, G., Geng, Q., Auerbach, A., & Li, F. (2020). Cell entry mechanisms of SARS-CoV-2. *Proceedings of the National Academy of Sciences, 117*(21), 11727–11734. https://doi.org/10.1073/pnas.2003138117

Shyr, Z. A., Gorshkov, K., Chen, C. Z., & Zheng, W. (2021). Drug discovery strategies for SARS-CoV-2. *Journal of Pharmacology and Experimental Therapeutics, 375*(1), 1–13. https://doi.org/10.1124/jpet.120.000212

Simmons, G., Reeves, J. D., Grogan, C. C., Vandenberghe, L. H., Baribaud, F., Whitbeck, J. C., ... & Bates, P. (2004). DC-SIGN and DC-SIGNR bind Ebola glycoproteins and enhance infection of macrophages and endothelial cells. *Virology, 305*(1), 115–123. https://doi.org/10.1016/j.virol.2002.12.029

Singh, A., & Chauthe, S. K. (2011). Entry inhibitors: Blocking HIV infection at the gate. *Biochimica et Biophysica Acta (BBA) - General Subjects, 1810*(11), 1108–1117. https://doi.org/10.1016/j.bbagen.2011.07.007

Skehel, J. J., & Wiley, D. C. (2000). Receptor binding and membrane fusion in virus entry: The influenza hemagglutinin. *Annual Review of Biochemistry, 69*, 531–569. https://doi.org/10.1146/annurev.biochem.69.1.531

Stertz, S., Reichelt, M., Spiegel, M., Kuri, T., Martínez-Sobrido, L., García-Sastre, A., ... & Weber, F. (2007). The intracellular sites of early replication and budding of SARS-coronavirus. *Virology, 361*(2), 304–315. https://doi.org/10.1016/j.virol.2006.11.027

Takada, A., Feldmann, H., Ksiazek, T. G., & Kawaoka, Y. (1997). Antibody-dependent enhancement of Ebola virus infection. *Journal of Virology, 71*(11), 8612–8619. https://doi.org/10.1128/jvi.71.11.8612-8619.1997

Trivedi, K., Mohan, M., & Byrareddy, S. N. (2020). Drug repurposing for COVID-19: Approaches, challenges and promising candidates. *Pharmacological Reports, 72*(6), 1479–1505. https://doi.org/10.1007/s43440-020-00155-8

Tulimilli, S., Sharma, A., Shukla, A., Gupta, A., Shukla, A., & Yadav, J. (2022). Structural biology of SARS-CoV-2 spike protein: Lessons learned for vaccine design. *Frontiers in Molecular Biosciences, 9*, 890. https://doi.org/10.3389/fmolb.2022.879014

Walls, A. C., Park, Y. J., Tortorici, M. A., Wall, A., McGuire, A. T., & Veesler, D. (2020). Structure, function, and antigenicity of the SARS-CoV-2 spike glycoprotein. *Cell, 181*(2), 281–292.e6. https://doi.org/10.1016/j.cell.2020.02.058

Whitt, M. A. (2010). Generation of VSV pseudotypes using recombinant ΔG-VSV for studies on virus entry, identification of entry inhibitors, and immune responses to vaccines. *Journal of Virological Methods, 169*(2), 365–374. https://doi.org/10.1016/j.jviromet.2010.08.006

WHO. (2020). Novel Coronavirus (2019-nCoV) Situation Report—1. World Health Organization.https://www.who.int/docs/default-source/coronaviruse/situation-reports/20200121-sitrep-1-2019-ncov.pdf

Wool-Lewis, R. J., & Bates, P. (1998). Characterization of Ebola virus entry by using pseudotyped viruses: Identification of receptor-deficient cell lines. *Journal of Virology, 72*(4), 3155–3160. https://doi.org/10.1128/JVI.72.4.3155-3160.1998

Wu, C., Liu, Y., Yang, Y., Zhang, P., Zhong, W., Wang, Y., ... & Li, H. (2022). Analysis of therapeutic targets for SARS-CoV-2 and discovery of potential drugs by computational methods. *Acta Pharmaceutica Sinica B, 10*(5), 766–788. https://doi.org/10.1016/j.apsb.2020.02.008

Xia, S., Liu, Q., Wang, Q., Sun, Z., Su, S., Du, L., ... & Jiang, S. (2018). Middle East respiratory syndrome coronavirus (MERS-CoV) entry inhibitors targeting spike protein. *Virus Research, 194*, 200–210. https://doi.org/10.1016/j.virusres.2014.09.014

Xia, S., Zhu, Y., Liu, M., Lan, Q., Xu, W., Wu, Y., ... & Lu, L. (2020). Fusion mechanism of 2019-nCoV and fusion inhibitors targeting HR1 domain in spike protein. *Cellular & Molecular Immunology, 17*(7), 765–767. https://doi.org/10.1038/s41423-020-0374-2

Xiang, Y., Wu, Q., Liang, L., Zhang, J., & Li, Y. (2022). Pseudoviruses: New models for studying viral entry and screening inhibitors. *Viruses, 14*(2), 307. https://doi.org/10.3390/v14020307

Yang, J., Wang, W., Chen, Z., Lu, S., Yang, F., Bi, Z., ... & Zhu, F. (2020). A vaccine targeting the RBD of the S protein of SARS-CoV-2 induces protective immunity. *Nature, 586*(7830), 572–577. https://doi.org/10.1038/s41586-020-2599-8

Yang, R., Huang, B., A R, L., Li, W., Wang, W., Deng, Y., ... & Tan, W. (2021). Development and effectiveness of pseudovirus-based assays for SARS-CoV-2. *Viruses, 13*(10), 2062. https://doi.org/10.3390/v13102062

Yoo, J. H., Lee, S., & Lee, J. Y. (2015). Natural products and their derivatives as antiviral agents. *Journal of Microbiology, 53*(12), 855–865. https://doi.org/10.1007/s12275-015-5295-2

Yu, J., Qiao, Y., Li, H., Chen, C., Wu, S., Zhou, X., & Yang, H. (2023). Streptomyces secondary metabolites as potential antiviral agents: Current knowledge and future perspectives. *Frontiers in Pharmacology, 14*, 1123. https://doi.org/10.3389/fphar.2023.1123176

Zaki, S. R., & Goldsmith, C. S. (1999). Pathogenesis of Ebola virus infection. *Journal of Infectious Diseases, 179*(Suppl 1), S274–S281. https://doi.org/10.1086/514313

Zhen, W., Guo, J., Wang, Z., & Chen, W. (2023). Antiviral properties of Bacillus-derived metabolites against influenza. *Frontiers in Microbiology, 14*, 121214. https://doi.org/10.3389/fmicb.2023.121214

Zhu, N., Zhang, D., Wang, W., Li, X., Yang, B., Song, J., ... & Tan, W. (2020). A novel coronavirus from patients with pneumonia in China, 2019. *New England Journal of Medicine, 382*(8), 727–733. https://doi.org/10.1056/NEJMoa2001017

APPENDIX

APPENDIX 1: Cytotoxic concentrations (CC 50 values) determined from dose response curve.

Samples	CC-50 (µg/ml)
Compound 2	126.3
Compound 32	71.55
Compound 1	162.5
Compound 3	205.3
Compound 4	154.0
Compound 5	90.40
Compound 6	38.67
Compound 7	94.25
Compound 8	176.2
Compound 9	308.3
Compound 10	Unstable
Compound 11	128.8
Compound 12	128.1
Compound 13	25.43
Compound 14	172.2
Compound 15	185.4
Compound 16	183.6
Compound 17	162.5
Compound 18	98.67
Compound 19	173.5

Compound 20	50656
Compound 21	295.5
Compound 22	1.233e-010
Compound 23	117.0
Compound 24	165.2
Compound 25	176.6
Compound 26	50.87
Compound 27	25.39
Compound 28	62.16
Compound 29	156.3
Compound 30	114.4
Compound 31	156.3